THE UNIVERSITY OF MICHIGAN

COLLEGE OF ENGINEERING
Department of Electrical Engineering
Space Physics Research Laboratory

Scientific Report No. FS-2

THEORETICAL CONSIDERATIONS IN DESIGN OF AN IONOSPHERIC PROBE

Prepared on behalf of the project by

R. L. Boggess

UMRI Projects 2816-1, 2521

The research reported in this document has been sponsored by the Ballistics Research Laboratory, Aberdeen Proving Ground, Contract No. DA-20-018-509-ORD-103, Project No. DA-5B03-06-011 ORD (TB 3-0538), and the Geophysics Research Directorate of the Air Force Cambridge Research Center, Air Research and Development Command, under Contract No. AF 19(604)-1843, Project No. 7643.

administered by:

THE UNIVERSITY OF MICHIGAN RESEARCH INSTITUTE ANN ARBOR

February 1959

TABLE OF CONTENTS

LIST OF FIGURES

LIST OF FIGURES
(Concluded)

LIST OF SYMBOLS

A	area
A_c	cross-sectional area
A_{eff}	effective area
J_e	random electron current density
J_p	random positive-ion current density
J_n	random negative-ion current density
J	current density
N_e	number density of electrons
N_p	number density of positive ions
N_n	number density of negative ions
N_g	number density of gas molecules
V_o	voltage equivalent of temperature of the undisturbed plasma*
v_o	most probable velocity of the undisturbed plasma*
T_e	electron temperature
T_p	positive-ion temperature
T_n	negative-ion temperature
T_g	gas temperature
i_e	electron electrode current
i_p	positive-ion electrode current
i_n	negative-ion electrode current
i_t	total electrode current
I_n	normalized current
a	sheath radius
r	collector radius
s	sheath thickness, $a-r = s$
e	unit charge 1.602×10^{-19} coulombs
k	Boltzmann's gas constant 1.3803×10^{-23} joules/°K
m_e	mass of an electron 9.11×10^{-31} kilograms
m_p	mass of a positive ion
m_n	mass of a negative ion
m_g	mass of a gas molecule
V	voltage between the sheath edge and an electrode
δV	voltage between two electrodes of a bipolar probe
r_i	radius of influence
r_e	effective radius
P	constant $[(8\sqrt{\pi}\ \epsilon_o k)/9e^2]\ (T/Nr^2)$
α**	transcendental function of (a/r) for sphere
β**	transcendental function of (a/r) for cylinder
ϵ_o	dielectric constant of free space 8.854×10^{-12} farads/meter

*$1/2\ mv_o^2 = kT_o = eV_o$

**See W. G. Dow, Fundamentals of Engineering Electronics, John Wiley and Son, New York, 1952.

ABSTRACT

The general theory of a Langmuir probe is reviewed and extended with emphasis on spherical geometry. Numerical and graphical methods are provided for calculating the volt-ampere characteristic of a bi-polar probe. The volt-ampere characteristics of three electrode combinations are illustrated. A brief discussion of the practical and theoretical considerations which led to the choice of a particular configuration is included.

I. INTRODUCTION

For the past twelve years the Department of Electrical Engineering of The University of Michigan has been engaged in measuring various properties of the upper atmosphere through the use of several sounding rockets.* Four of these rockets have carried as a secondary experiment an elementary adaptation of the Langmuir probe for study of the ionosphere. The information obtained from the probe experiment on these flights indicated that this should become a useful upper-atmosphere measuring device. The design, however, was seriously compromised in each case by the primary experiment carried by the rocket and by the unknown surface condition of the rocket. A re-study of the practical aspects of the problems encountered indicates that advances in rocket instrumentation techniques and vehicles now make designs practical which would have been considered impractical previously. For example, the complete ejection of the instrumentation can now be done with confidence. In addition, advances in circuit components allow remarkable reduction in instrumentation size, thereby easing the ejection problem and allowing greater freedom in choice of geometry and size. This, in turn, reduces the problems encountered in the transition from theory to practice.

The experience gained from the previous firings, combined with a review of basic probe theory and its extension in some areas, has led to the design of a specific probe instrumentation. One was carried aloft by a Nike-Cajun rocket October 20, 1958, followed by a second instrumentation on a Spaerobee, November 30, 1958.

II. HISTORICAL OUTLINE

In 1901, when Marconi proved that radio waves could be received across the Atlantic Ocean, he thereby demonstrated that the earth was not, as had been previously thought, surrounded by free space. In the following year, the existence of an ionized region was independently postulated by Heaviside and Kennelly.

---

*The earlier work in conjunction with V-2 rockets was supported by Air Materiel Command, Air Force Cambridge Research Laboratories (AFCRL), Contract No. AF 19(122)-55. Probe study was resumed with the support of the Geophysics Research Directorate, Air Force Cambridge Research Center (AFCRC), Contract No. AF 19(604)-1843. This latter contract supports the present probe investigations jointly with Ballistic Research Laboratory, Aberdeen Proving Ground, Contract No. DA-20-018-509-ORD-103, Project No. DA 5B03-06-011 ORD (TB 3-0538).

This hypothesis was confirmed experimentally in 1925 by Appleton and Barnett, who measured arrival angles of waves transmitted from a distant transmitter. It was demonstrated that the waves came from an elevated angle and thus were "sky" waves. By 1926, the "radar" technique of short vertical pulse soundings had been devised by Bret and Tuve, and thus man's study of the ionosphere was initiated.

As study of the ionosphere has progressed through the years, many refinements in sounding equipment have been made. With each refinement it has become possible to learn more of the complex nature of the ionosphere, thereby drawing attention to the need for a more direct type of measurement (preferably point-by-point), capable of determining fine detail rather than grosser aspects.

It became possible to conduct direct measurements when V-2 rockets were available shortly after World War II. It was quite natural that probe techniques, used in the study of gaseous discharge tubes, should be considered in connection with measuring properties of the ionosphere. It was at this time that a probe experiment was included in the instrumentation being prepared for V-2 flights in connection with a contract between The University of Michigan and the Air Materiel Command of the U. S. Air Force. (A quite different method, based on the relative delay of two rf signals, was also carried out on early rocket flights by The University of Michigan and AFCRC, and also by the Naval Research Laboratory.[1-4])

Probes were placed on three successful V-2 flights in 1946 and 1947. The results of these flights were reported in detail in several articles and reports.[5-8] Unfortunately, since the location and shape of the probes were dictated to a great extent by the other instruments being flown, they were awkward in design. This resulted in a great deal of uncertainty in the data because

(a) the probes did not approximate any ideal geometry, such as a cylinder or sphere;
(b) the sheaths of the electrodes overlapped; and
(c) thermal equilibrium was disturbed in an unknown manner due to the velocity of the rocket through the ionosphere.

But results, however ambiguous, did indicate that the experiment could become a valuable tool for measuring properties of the ionosphere.

At this time, however, interest was greater in carrying out studies of the lower rather than the upper regions of the upper atmosphere and support for the probe experiment faltered. Consequently, no further investigations were carried out for several years.

The University of Michigan remained interested in the probe experiment and, following the development of the Aerobee-Hi rocket, which is capable of lifting an instrument load well into the ionosphere, study was resumed.* This involved

*Sponsored by the Geophysics Research Directorate of the Air Force Cambridge Research Center, AF 19(604)-1843.

a review of the earlier work in the light of then present knowledge of the ionosphere and additional theoretical considerations.

Following this study, additional support allowed the development and launching of an elementary probe as a secondary experiment on a rocket instrumented primarily to measure pressure, temperature, and density (separate contract with AFCRC). This experiment utilized a sphere (extended from the rocket) as one electrode and the main rocket body as a second electrode. But partially due to failure of the spherical electrode to become extended adequately, the experiment suffered from many of the problems noted previously. Thus the ideas previously held, that the probe geometry must be carefully controlled, and that ejection of the probe instrument is essential to permit a nearly ideal experiment, were largely confirmed.

In the laboratory, thin cylindrical electrodes or small planar surfaces are usually preferred for their geometrical convenience. In the ionosphere, however, a sphere has several advantages due to its symmetry. It is therefore desirable to reconsider the theoretical basis for the experiment in the light of the possibility of achieving isolation of an instrument in the ionosphere, with particular emphasis upon spherical geometries. The following sections of this report are thus devoted primarily to development of theoretical aspects of the experiment.

III. THEORETICAL DEVELOPMENT

When a small exploring electrode is placed in an ionized gas, it is surrounded by a space-charge region which is commonly referred to as the sheath. This electrode may be either a conductor or a nonconductor, but for the purposes of this report it is considered to be a conductor. If the electrode is allowed to assume a potential that is determined only by the properties of plasma, it must assume a potential with respect to the plasma such that the net current to the electrode is zero. In general, this potential, which is referred to as the wall potential, will be negative with respect to the plasma.

If the potential of the electrode is changed in some manner from this wall potential, a current will result. The current will be determined by the voltage across the sheath, the velocity of the ions and electrons arriving at its edge, and its dimensions. The current, however, is nearly independent of the potential distribution within the sheath, whose potential distribution and thickness depends upon space-charge considerations. Neither the potential difference between the plasma and the electrode nor the initial velocities of the charge carriers play an important role in this latter regard.

For the purpose of mathematical convenience, it is desirable to define several boundaries in the region surrounding the electrode (Fig. 1). These are:

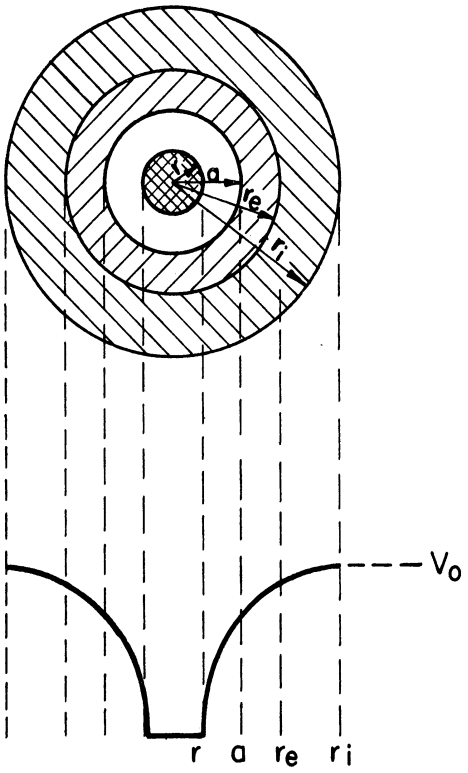

Fig. 1. Potential distribution, and boundaries of regions surrounding an electrode.

(a) electrode radius r,
(b) sheath boundary a,
(c) sphere of influence of radius r_i, and
(d) effective sphere radius r_e.

The region between r and a, the sheath, has a positive-ion space charge and will be referred to as a positive-ion sheath. In general, the region is considered to have a negligible number of electrons.

The sheath thickness can be measured accurately by optical means in the laboratory when the probe technique is used for gas-discharge tube studies. Other plasma parameters, such as gas temperature, composition, etc., are also measurable in a laboratory application, and thus certain aspects of the theory can be checked.

The region of influence (bounded by r_i) is that region of the plasma altered by the existence of the electrode. In the more elementary theoretical approach, it is assumed to correspond to the sheath, but may be defined as a region larger than the sheath. In this instance, Boltzmann's relations are assumed to apply in the region not considered sheath. The Debye length[9] may serve as a convenient unit of measure in this region.

A spherical electrode collects more positive ions by virtue of its negative charge than an uncharged sphere of equal size. A larger sphere, uncharged, may be defined such that the random current collected is equivalent to that collected by the smaller charged sphere. This hypothetical sphere is referred to herein as having an effective radius r_e. It must be less than the radius of influence.

The region between r_i and a is a transition region from the undisturbed plasma to the sheath. The voltage across this region is usually small and can be neglected. A sketch of a potential distribution in which the transition region is exaggerated is also shown in Fig. 1.

A. ELEMENTARY SOLUTION

Consider now a negatively charged spherical electrode and its "spherical region of influence" of radius r_i lying in a region containing positive ions. When the radius of influence is large compared with the electrode radius, and the velocity of the ions is appreciable at the boundary of the region of influence, orbital motion of the ions must be considered in determining the current to the electrode. Referring to Fig. 2, AB predicts the path of an uninfluenced

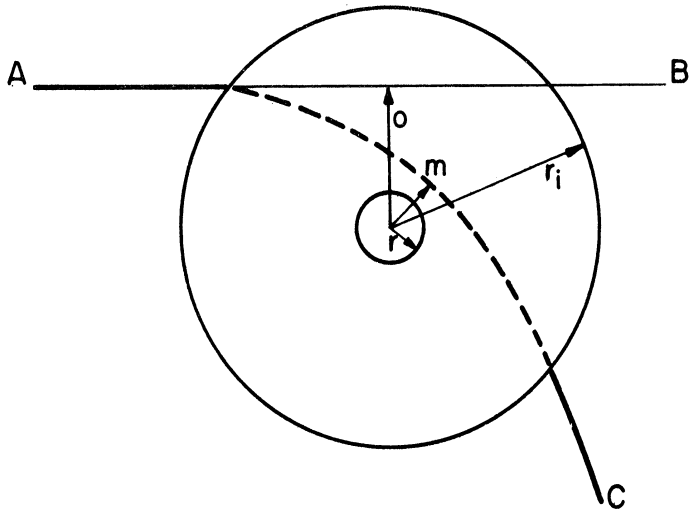

Fig. 2. Positive-ion trajectory about a negative spherical electrode.

ion and AC depicts the path of an orbiting ion. It is assumed that no collisions occur. One can calculate the behavior of an ion in the "sphere of influence" using the law of conservation of angular momentum and the law of conservation of energy.

The kinetic energy gained by the ion in passing from a point on r_i to the point m is given by

$$1/2\ mv^2 = e(V_o - V_m) \quad , \tag{1}$$

where V_o is the potential at point o (undisturbed plasma) and V_m is the potential at point m. The conservation of angular momentum demands that

$$mr_o v_o = mr_m v_m \quad , \tag{2}$$

where r_o is the distance to point o, v_o is the uninfluenced velocity, r_m is the distance to point m, and v_m is the velocity at point m. By manipulation of Eqs. (1) and (2) and letting $V = V_m - V_o$, it can be shown that

$$r_o = r_m \sqrt{1 + \frac{V}{V_o}} \quad . \tag{3}$$

If the value of $r_m \leq r$, the ion will strike the probe or just graze it and, for the purposes of this report, will be considered collected. In this case, r_m is effectively r, and r_o can be interpreted as r_e, the effective radius, allowing Eq. (3) to be written as

$$r_e = r\sqrt{1 + \frac{V}{V_o}} \tag{4}$$

Equation (5) may be used to determine, for example the current to a sphere in a region where all the ions have equal velocities and the same direction with respect to the electrode. This situation may in effect be encountered in rocket applications when the electrode velocity is very high with respect to the ion velocity. When the electrode velocity is sufficiently great, the actual velocity distribution of the ions is unimportant.

The random ion current density may be written

$$J_p = N_p v_p \quad , \tag{5}$$

where J_p is the positive-ion current density, N_p is the number density of the ions, and v_p is the most probable ion velocity. The current, i_p, to the electrode then will equal to the random current density times its effective cross-sectional area:

$$i_p = J_p \pi r_e^2 \quad . \tag{6}$$

Substituting Eq. (4) into Eq. (6):

$$i_p = J_p A_c \left(1 + \frac{V}{V_o}\right) \quad , \tag{7}$$

where $A_c = \pi r^2$. The corresponding expression for a unit length of a cylinder whose axis lies perpendicular to the direction of the ions is

$$i_p = J_p A_c \sqrt{1 + \frac{V}{V_o}} \quad , \tag{8}$$

where A_c is the projected area of the cylinder, $2\pi rl$. Figure 3 is a sketch of the variation of i_p vs. V for (1) a sphere, (2) a cylinder, and (3) a plane.

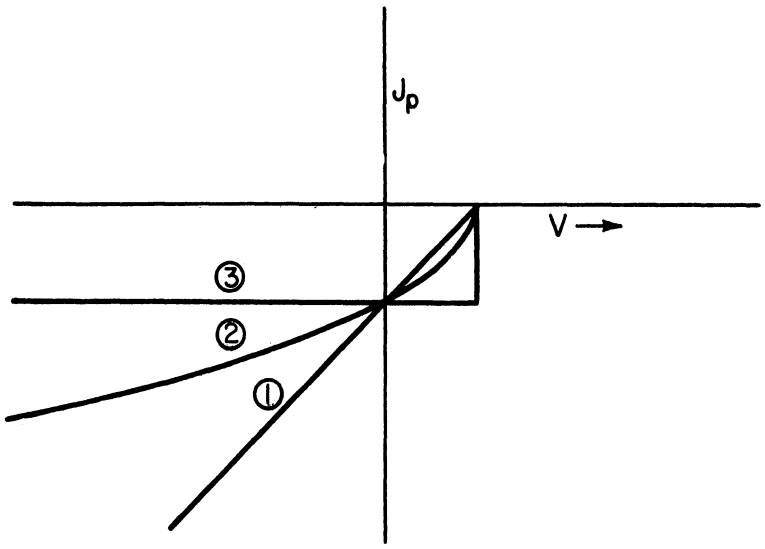

Fig. 3. Electrode volt-ampere characteristics for unidirectional energy distribution.

If all ions have the same velocity but are random in direction, then the entire surface of the electrode is effective. In this case the total area rather than the cross-sectional area of the electrode applies. Thus Eqs. (9) and (10) are obtained corresponding to (7) and (8), respectively.

$$i_p = J_p A \left(1 + \frac{V}{V_o}\right) \tag{9}$$

$$i_p = J_p A \sqrt{1 + \frac{V}{V_o}} \tag{10}$$

Figure 3 also represents this situation since only the scale is different.

B. GENERAL SOLUTION

The above elementary solution does not consider the effect of the space-charge region (sheath) or the energy-distribution function of the particles. A more general solution is necessary.

As noted previously, if a spherical electrode is immersed in a uniformly ionized region, it will be surrounded by a concentric spherical positive-ion sheath of radius a. The region of influence is assumed to correspond to the sheath edge ($r_i = a$), that is, the potential at the sheath edge is assumed to be equal to the potential of the undisturbed plasma.

Consider the outer edge of the sheath in terms of a right-hand cartesian coordinate system with u the radially directed velocity component and tangent velocity components v and w. The velocity u is considered positive when directed toward the center of the sphere (see Figure 4).

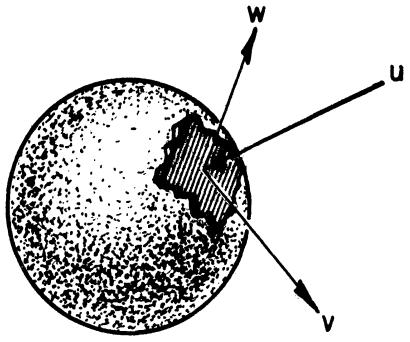

Fig. 4. Velocity-space coordinate system at sheath edge.

If the number of ions N_p at the sheath edge in an incremental volume, $d\tau$, has a velocity distribution

$$f(u,v,w)dudvdw \quad , \tag{11}$$

then

$$N_p f(u,v,w)dydvdwd\tau \tag{12}$$

is the number of ions that can be expected to have velocities lying in the ranges u to u + du, v to v + dv, and w to w + dw. The number of ions that can be expected to cross the spherical sheath boundary per unit time of the ions within the velocity limits given is

$$4\pi a^2 N_p uf(u,v,w)dudvdw \tag{13}$$

This assumes uniform ionization and velocity distribution throughout the region of influence.

The total current crossing the boundary is then obtained by multiplying Eq. (13) by the ionic charge (e) and integrating between the proper limits. Thus

$$i_p = 4\pi a^2 N_p e \int_{o,u_1}^{\infty} \int_{-v_1}^{+v_1} \int_{-w}^{+w} uf(u,v,w)dw,dv,du \tag{14}$$

The lower limit u applies for a retarding potential on the probe, and the lower limit zero applies for an accelerating potential.

If a Maxwellian distribution is assumed, it may be expressed in cartesian coordinates as

$$f(u,v,w) = \left(\frac{m}{2\pi kT}\right)^{3/2} \exp\left[-\frac{m}{2kT}(u^2+v^2+w^2)\right] \quad , \tag{15}$$

where k is Boltzmann's constant and T is the absolute temperature in °K. However, it is convenient to transform Eq. (15) using

$$u = u, \; v = p \sin\theta, \; w = p \cos\theta \quad ,$$

where u is the velocity component normal to the sheath, p is the corresponding tangential component and θ is the angle between p and an arbitrary reference. Thus the Maxwellian distribution may be written

$$f(u,p) = \left(\frac{m}{2kT}\right)^{3/2} \frac{1}{\sqrt{2\pi}} \exp - \frac{m}{2kT}(u^2+p^2)dudp \quad . \tag{16}$$

Equation (14) may be written in terms of the new variables, and upon using Eq. (16) to express the distribution function, the following results:

$$i_p = \frac{4\pi a^2}{\sqrt{2\pi}} N_p e \int_{u_1}^{\infty} \int_{0}^{p_1} u_p \left(\frac{m}{2\pi kT}\right)^{3/2} \exp\left[-\frac{m}{2kT}(u^2+p^2)\right] dp\,du. \quad (17)$$

The limits u_1 and p_1 are dependent upon the orbital motion of the ions within the sheath. Thus they are determined by the laws of angular momentum and conservation of energy. The resulting expressions are

$$u_1^2 = -2\frac{e}{m_p}V \quad (18)$$

and

$$p_1^2 = \frac{r^2}{a^2-r^2}\left(U^2+2\frac{e}{m_p}V\right) \quad (19)$$

Using Eqs. (18) and (19) as limits in solving Eq. (17), the following is obtained:

$$i_p = 4\pi r a^2 \sqrt{\frac{kT}{2\pi m}} N_p e \left[1-\frac{a^2-r^2}{a^2}\exp-\frac{eV}{kT}\left(\frac{r^2}{a^2-r^2}\right)\right]. \quad (20)$$

If V_o represents the voltage equivalent of temperature,

$$\frac{eV}{kT} = \frac{V}{V_o}. \quad (21)$$

Substituting Eq. (21) in Eq. (20) and rearranging

$$i_p = A N_p e \sqrt{\frac{kT_p}{2\pi m_p}}\left\{\frac{a}{r}-\left(\frac{a^2-r^2}{r^2}\right)\exp\left[-\left(\frac{V}{V_o}\right)\left(\frac{r^2}{a^2-r^2}\right)\right]\right\}. \quad (22)$$

Equation (22) is the current to the electrode, when the potential is accelerating [lower limit $u = u_1$ in Eq. (14)].

In the case of a retarding potential [lower limit $u = 0$ in Eq. (14)],

$$i_p = A N_p e \sqrt{\frac{kT_p}{2\pi m_p}} \exp\left(\frac{V}{V_o}\right) \quad (23)$$

The total current entering the sheath (not all ions are collected) may be calculated by integrating Eq. (17) over all velocities. Thus

$$J_p = N_p e \int_0^{\infty}\int_0^{\infty} u_p f(u_1 p)\,du\,dp \quad (24)$$

becomes, for the Maxwellian distribution,

$$J_p = N_p e \sqrt{\frac{kT}{2\pi m_p}} \quad . \tag{25}$$

This is the random ion current crossing a unit area of the sheath. It represents an isotropic current density in a region where the velocity is everywhere Maxwellian. This is actually not the case at the sheath edge since in general more ions enter the sheath than leave it. In an extreme case all the ions enter the sheath and none leave it, as will be demonstrated later in the case of sheath-area-limited current. The validity of the assumption made here, of a Maxwellian distribution, has been demonstrated on many occasions.[9] It is convenient to normalize Eqs. (22) and (23), letting

$$I_{np} = \frac{i_p}{AJ_p} \quad . \tag{26}$$

This is a normalized current and is the ratio of the current to the electrode in the presence of a sheath, to the current in the absence of a sheath. Using Eqs. (25) and (26), Eq. (22) becomes

$$I_{np} = \left(\frac{a}{r}\right)^2 - \left(\frac{a^2-r^2}{r^2}\right) \exp -\left(\frac{V}{V_o}\right)\left(\frac{r^2}{a^2-r^2}\right) \tag{27}$$

for accelerating potential,

$$\left(\frac{V}{V_o}\right) > 1 \quad ,$$

and Eq. (23) becomes

$$I_{np} = \exp\left(\frac{V}{V_o}\right) \tag{28}$$

for retarding potential,

$$\left(\frac{V}{V_o}\right) < 1 \quad .$$

In the latter case, the current is independent of the sheath dimensions, and its logarithm is a linear function of the collector potential. This is fortunate, as it permits the determination of the temperature of the charge carriers independent of many ionospheric parameters.

In the case of an accelerating potential, the current is dependent on the sheath radius and thus requires another independent equation to make the calculation possible. This equation can be determined from relationships defining space-charge-limited flow in a spherical system, which is

$$i = \frac{4\sqrt{2}}{9} \pi \epsilon_o \sqrt{\frac{e}{m}} \frac{V^{3/2}}{-\alpha^2} , \tag{29}$$

where α is a transcendental function of (a/r) that has been plotted in Fig. 5, and ϵ_o is the dielectric constant of free space. When normalized according to Eqs. (25) and (26),

$$I_{np} = \frac{P}{-\alpha^2}\left(\frac{V}{V_o}\right)^{3/2} , \tag{30}$$

where

$$P = \frac{8\sqrt{\pi}\,\epsilon_o k}{9e^2} \frac{T}{Nr^2} = 7.51 \times 10^3 \frac{T}{Nr^2} . \tag{31}$$

In developing Eq. (29), no initial random velocity of the ions was assumed. A correction for a Maxwellian distribution may be made by substituting

$$V^{3/2}\left(1 + 0.0247\sqrt{\frac{T}{V}}\right) \text{ for } V^{3/2} .$$

Equations (27) and (31) form, with $f(a/r) = -\alpha^2$, a transcendental system of equations which in general permit only numerical or graphical solutions. If Eq. (27) is plotted on log-log coordinates as a family of curves with (a/r) as the parameter (Fig. 6), then a particular solution of Eq. (31) would appear as a straight line with a slope of 3/2 in the same coordinates. Thus the intersection of a solution of Eq. (32) (straight line) with a solution of Eq. (28) (curve) for a particular (a/r) is a simultaneous solution of the two equations. A curve through a series of such intersections for a given temperature, number density, and electrode size is the volt-ampere characteristic of the electrode. In making calculations, Figs. 7-13, which are enlarged sections of Fig. 6, were used.

C. APPROXIMATIONS OF THE GENERAL SOLUTION

Often an approximate solution is all that is required in a preliminary study of a particular electrode design. Thus one of three appropriate simpler relations may be used. Two of these are asymptotic solutions of Eq. (27), while the third approximates the numerical solution of Eq. (27) and Eq. (30) in the form of one of the asymptotic solutions.

The first asymptotic solution applies in the case of either low ion density, small collector radius, or high temperature. In this case, the sheath is thick ($a/r \to \infty$). Thus the numerical solutions are asymptotic to the $(a/r) = \infty$ curve in Fig. 6. This is determined mathematically by expanding Eq. (27) as a power

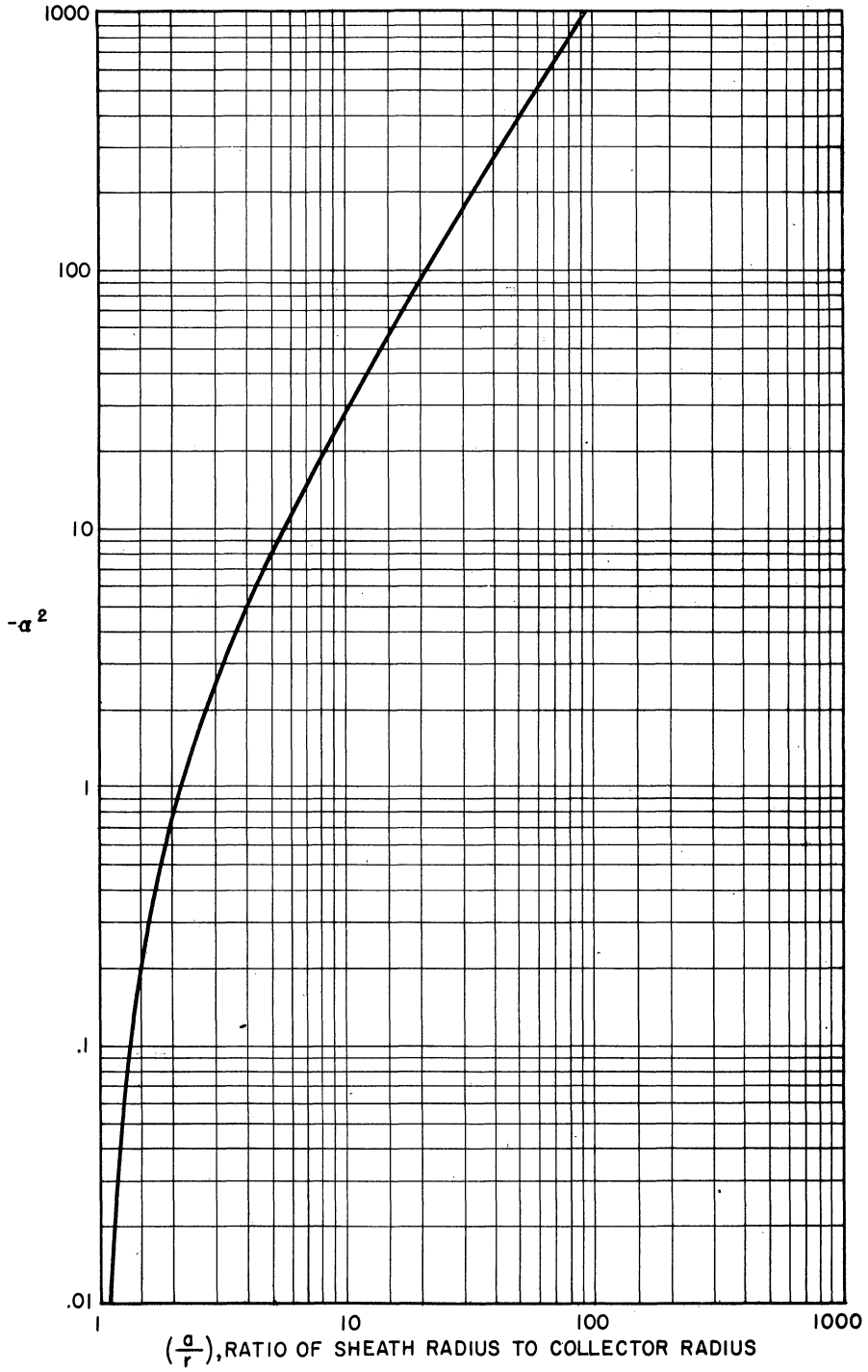

Fig. 5. $-\alpha^2$ vs. (a/r), ratio of sheath radius to collector radius.

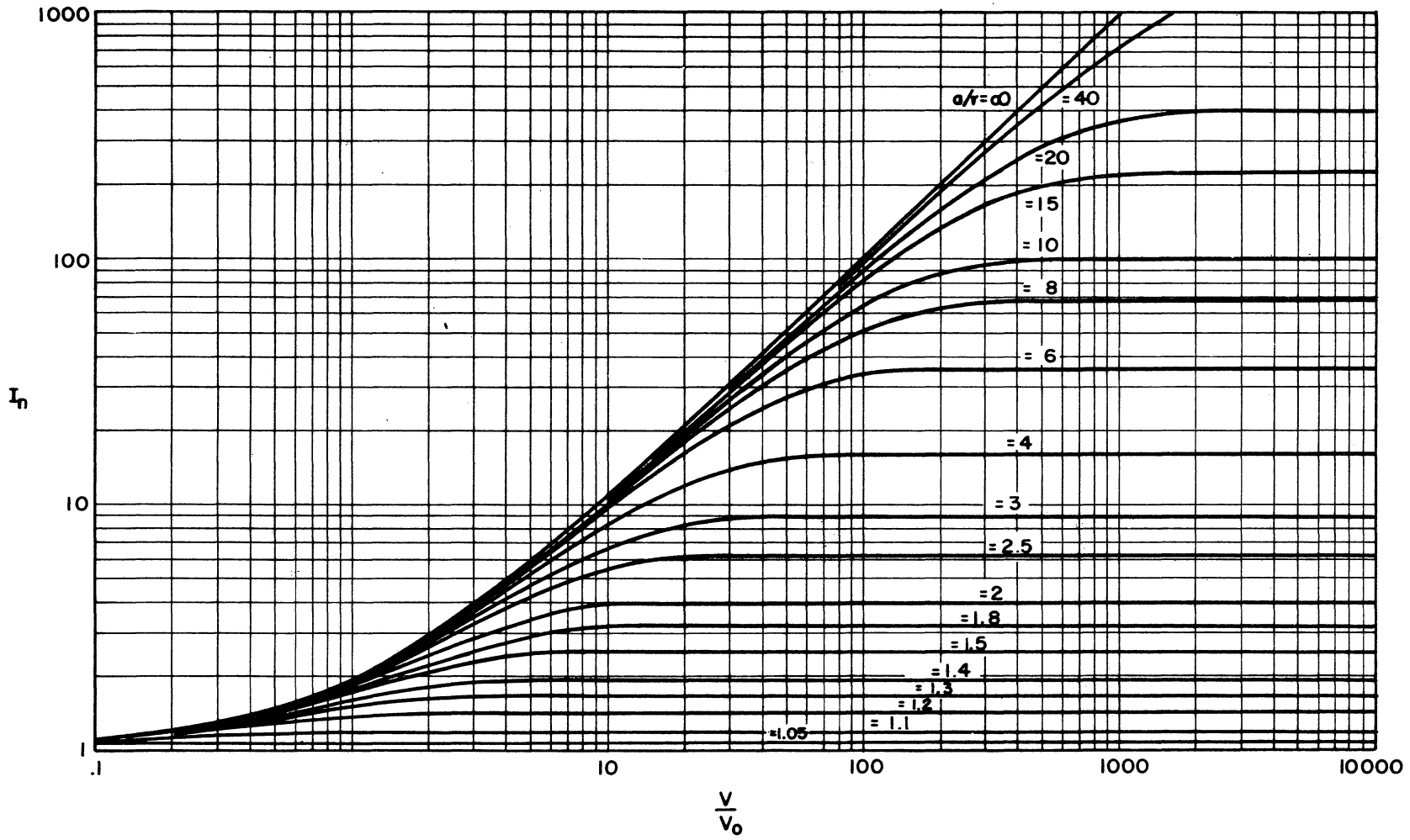

Fig. 6. Normalized current for a spherical electrode. $1 < I_n < 1000$; $0.1 < V/V_o < 10{,}000$.

$$I_n = \left(\frac{a}{r}\right)^2 - \left(\frac{a^2-r^2}{r^2}\right) \exp - \left(\frac{V}{V_o}\right)\left(\frac{r^2}{a^2-r^2}\right)$$

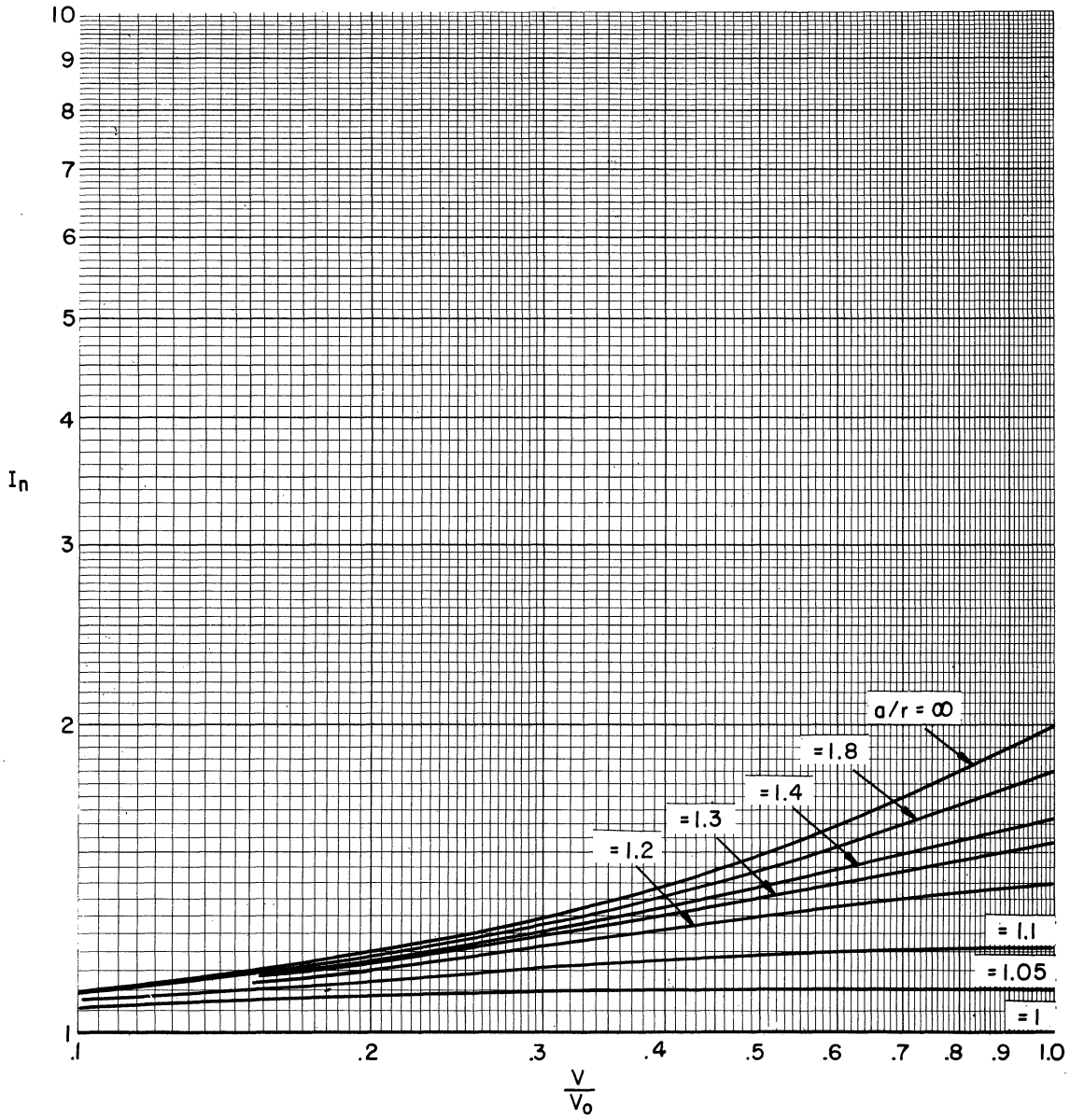

Fig. 7. Normalized current for a spherical electrode. $1 < I_n < 10$; $0.1 < V/V_o < 1$.

$$I_n = \left(\frac{a}{r}\right)^2 - \left(\frac{a^2-r^2}{r^2}\right) \exp - \left(\frac{V}{V_o}\right)\left(\frac{r^2}{a^2-r^2}\right)$$

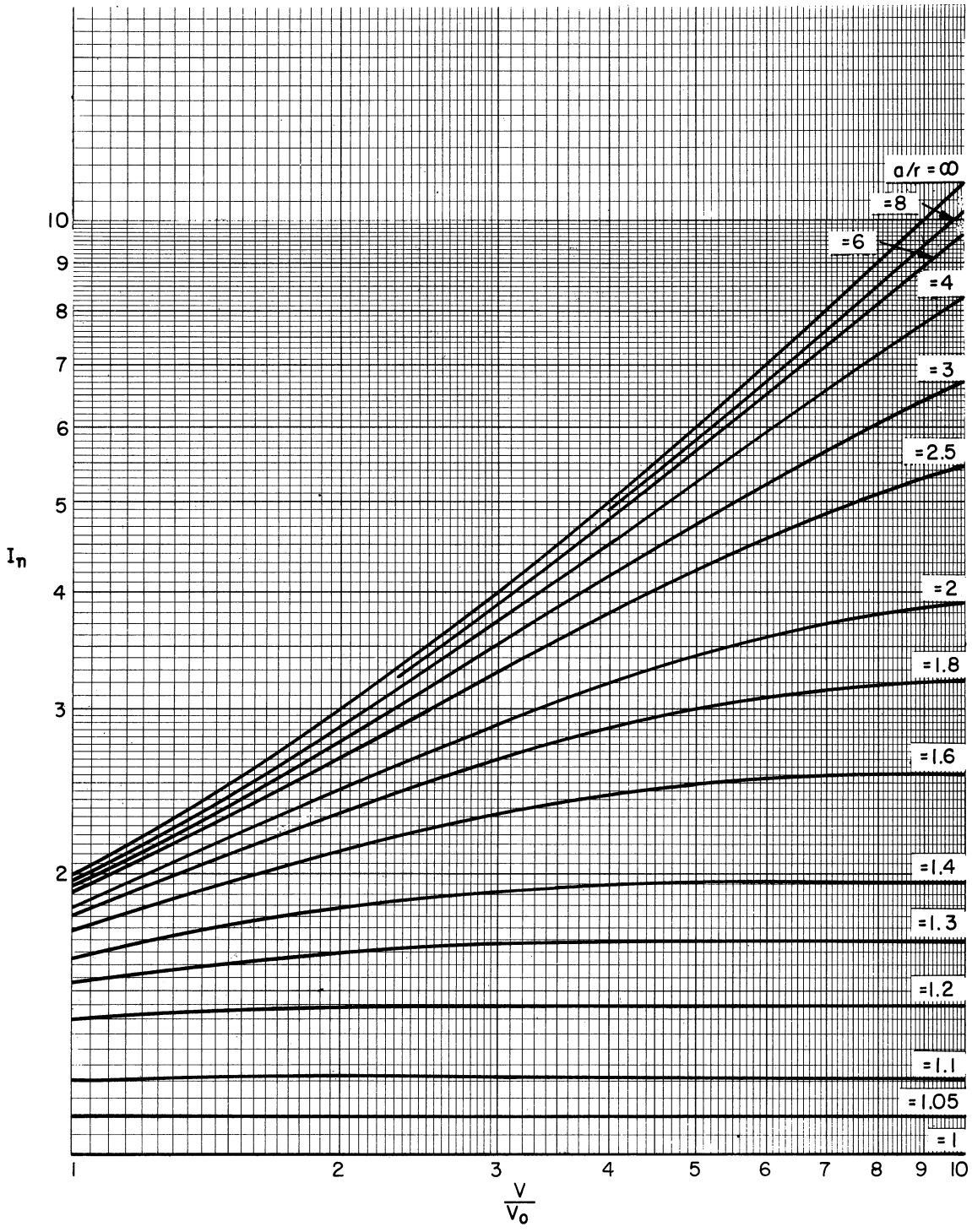

Fig. 8. Normalized current for a spherical electrode. $1 < I_n < 10$; $1 < V/V_o < 10$.

$$I_n = \left(\frac{a}{r}\right)^2 - \left(\frac{a^2-r^2}{r^2}\right) \exp - \left(\frac{V}{V_o}\right)\left(\frac{r^2}{a^2-r^2}\right)$$

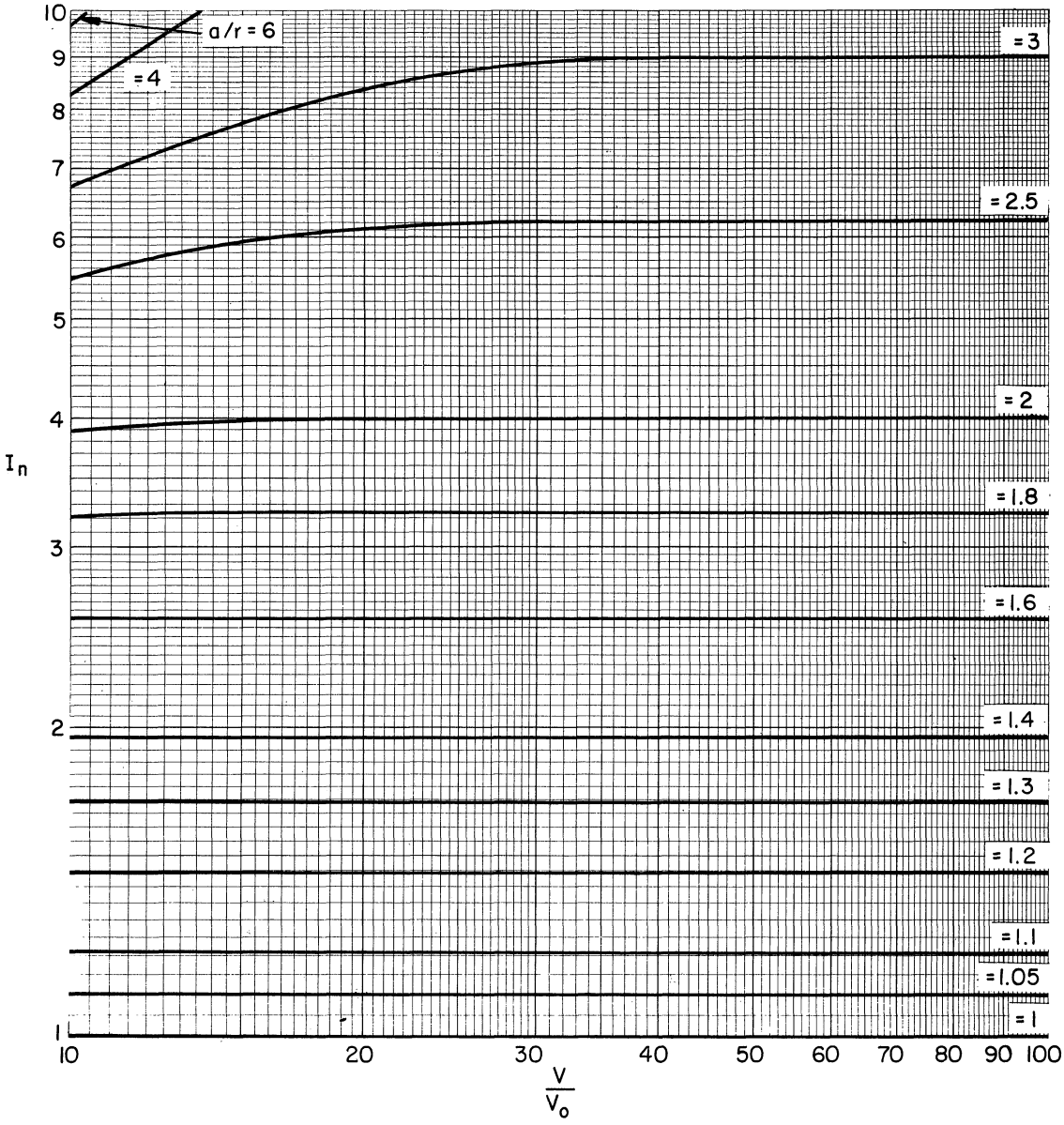

Fig. 9. Normalized current for a spherical electrode. $1 < I_n < 10$; $10 < V/V_o < 10^2$.

$$I_n = \left(\frac{a}{r}\right)^2 - \left(\frac{a^2-r^2}{r^2}\right) \exp - \left(\frac{V}{V_o}\right)\left(\frac{r^2}{a^2-r^2}\right)$$

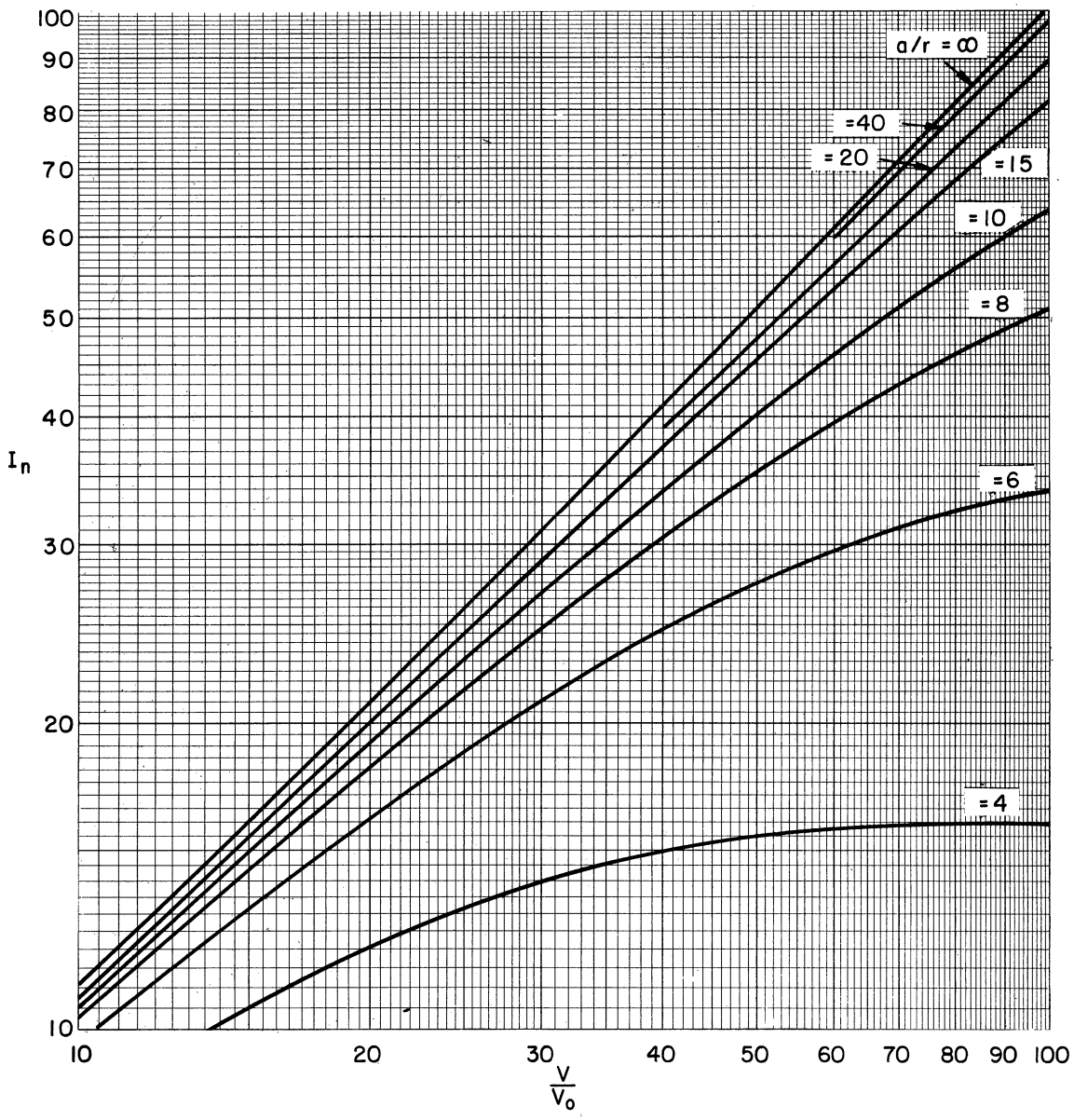

Fig. 10. Normalized current for a spherical electrode. $10 < I_n < 10^2$; $10 < V/V_o < 10^2$.

$$I_n = \left(\frac{a}{r}\right)^2 - \left(\frac{a^2-r^2}{r^2}\right) \exp - \left(\frac{V}{V_o}\right)\left(\frac{r^2}{a^2-r^2}\right)$$

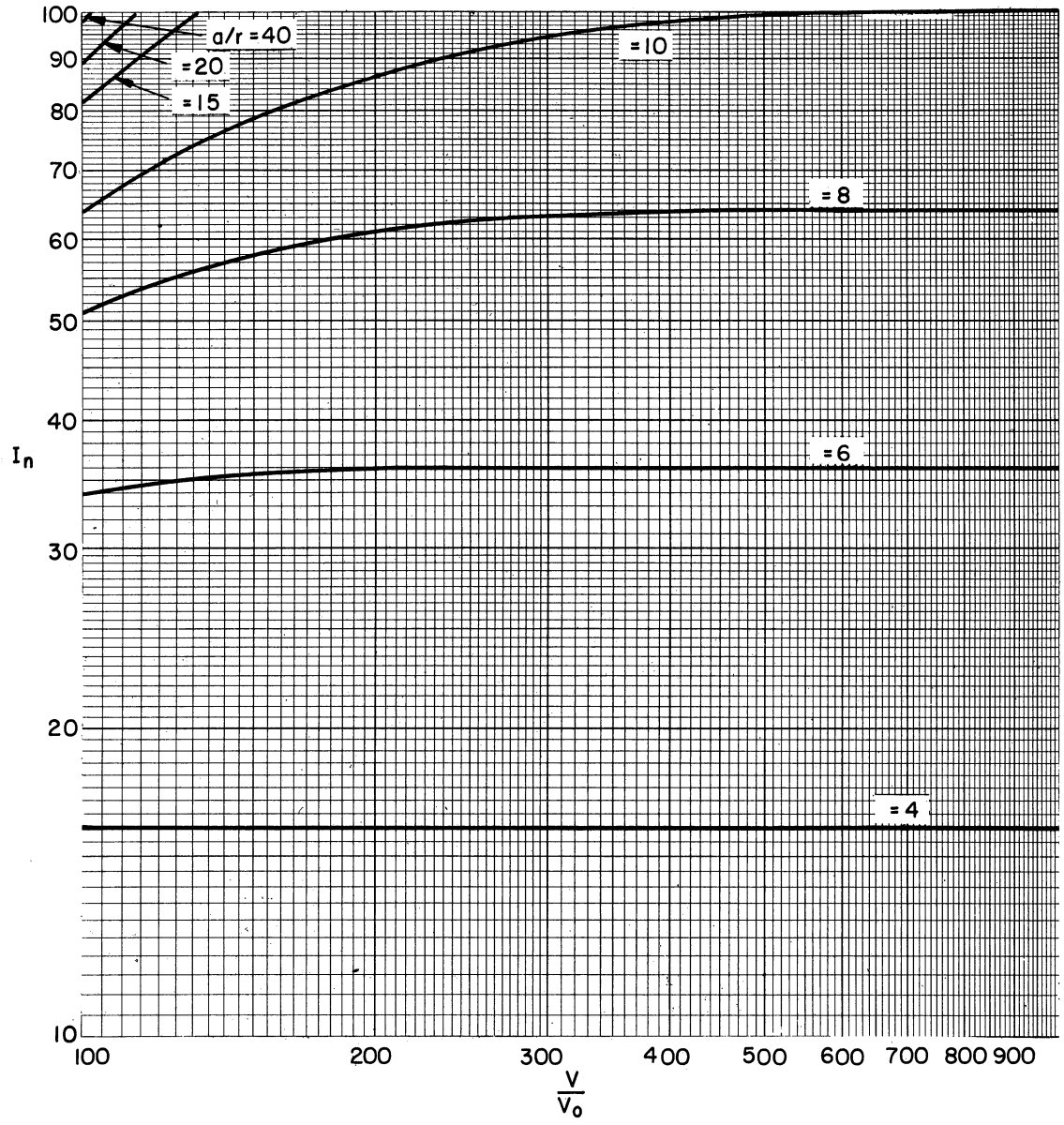

Fig. 11. Normalized current for a spherical electrode. $10 < I_n < 10^2$; $10^2 < V/V_o < 10^3$.

$$I_n = \left(\frac{a}{r}\right)^2 - \left(\frac{a^2-r^2}{r^2}\right) \exp - \left(\frac{V}{V_o}\right)\left(\frac{r^2}{a^2-r^2}\right)$$

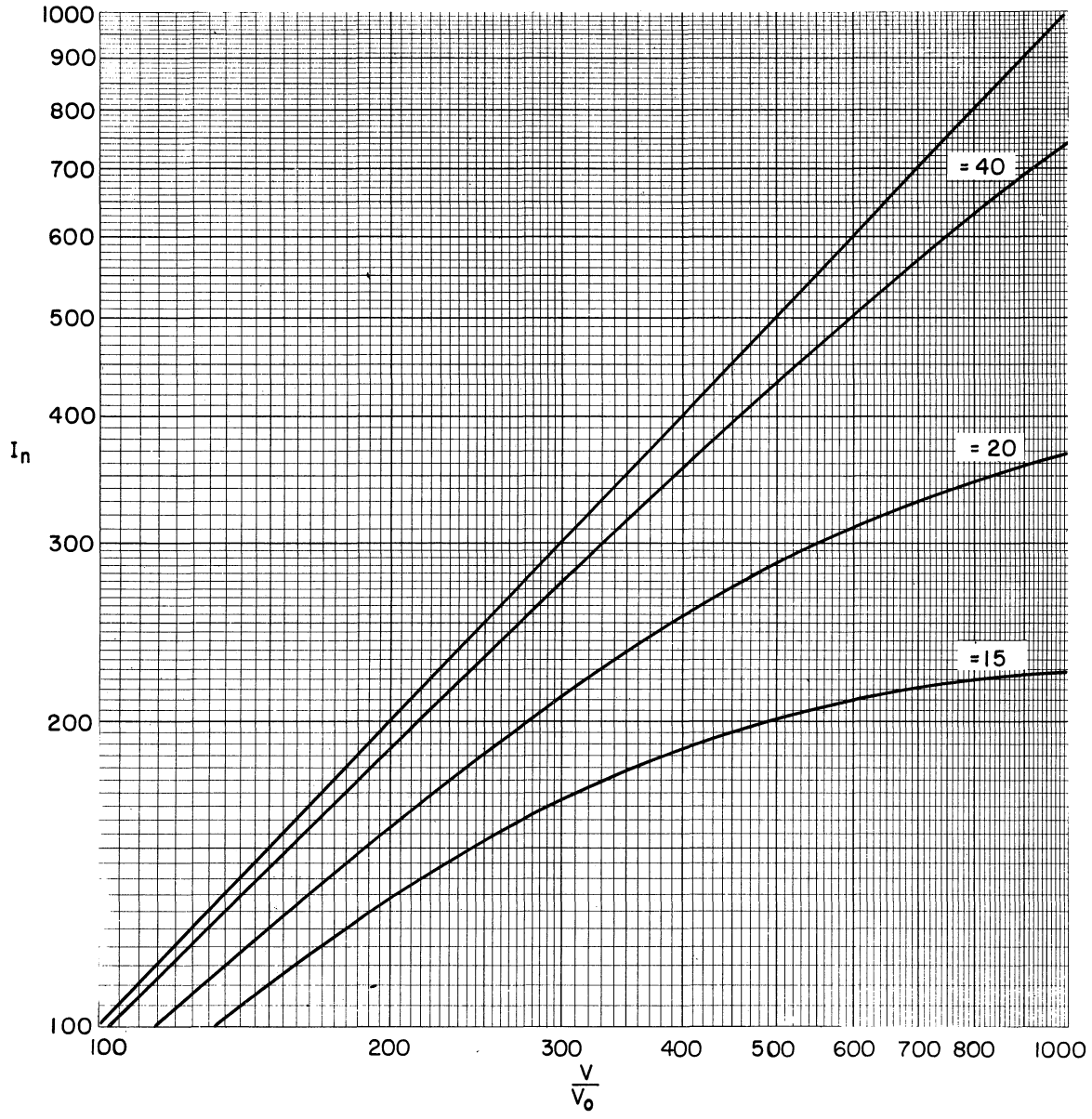

Fig. 12. Normalized current for a spherical electrode. $10^2 < I_n < 10^3$; $10^2 < V/V_o < 10^3$.

$$I_n = \left(\frac{a}{r}\right)^2 - \left(\frac{a^2-r^2}{r^2}\right) \exp - \left(\frac{V}{V_o}\right)\left(\frac{r^2}{a^2-r^2}\right)$$

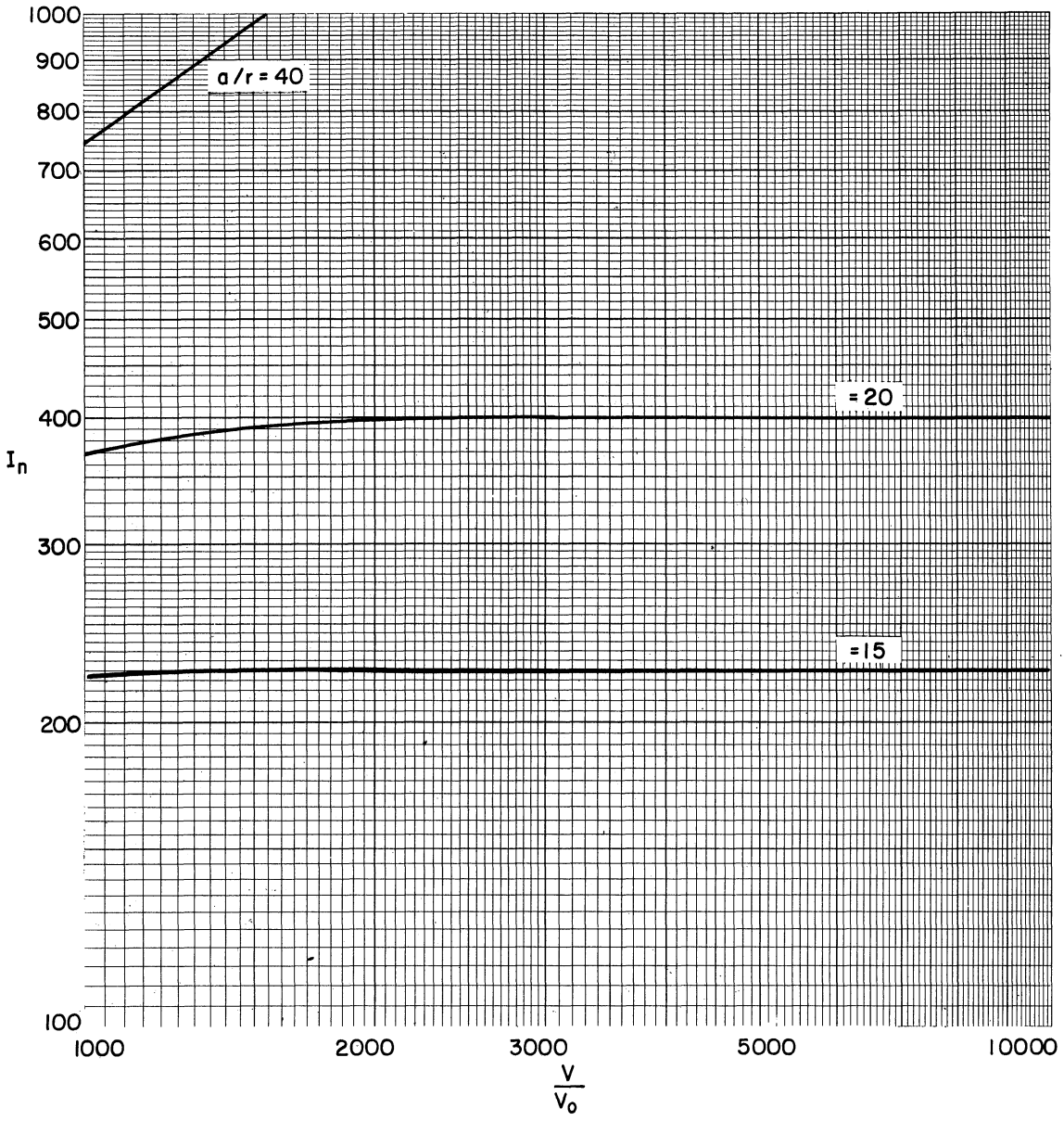

Fig. 13. Normalized current for a spherical electrode. $10^2 < I_n < 10^3$; $10^3 < V/V_o < 10^4$.

$$I_n = \left(\frac{a}{r}\right)^2 - \left(\frac{a^2-r^2}{r^2}\right) \exp - \left(\frac{V}{V_o}\right)\left(\frac{r^2}{a^2-r^2}\right)$$

series and allowing (a/r) to approach infinity. The result is

$$I_{np} = \left(1 + \frac{V}{V_o}\right) \tag{32}$$

for

$$\left(\frac{V}{V_o}\right) > 2$$

This is called the orbital-motion-limited solution since the current is dependent on the motion of the ions within the sheath. It is interesting to note that this is the normalized form of Eq. (9) which was obtained in the case of an equal-velocity randomly directed energy distribution.

The second asymptotic solution applies in the case of either low ion temperature, high ion density, or large collector radius. In this case, the sheath is thin ($a/r \to 1$) and Eq. (27) reduces to

$$I = \left(\frac{a}{r}\right)^2 . \tag{33}$$

All ions arriving at the sheath are collected and the current is dependent only on the sheath area. Thus this is termed the sheath-area-limited current.

Equations (32) and (33) are very useful, but occasionally it is necessary to consider an intermediate case, neither sheath-area-limited nor orbital-motion-limited. It is thus desirable to obtain an approximate solution for this intermediate case.

When Eqs. (27) and (30) are combined with the relation between $-\alpha^2$ and (a/r), a family of curves may be generated with P [see Eq. (31)] as the parameter. Figure 14 compares the solutions of a spherical electrode, when P = 0.666 and P = 0.1, with the orbital-motion-limited solution. It is seen that the curves have approximately the same curvature but are displaced horizontally by an amount depending on P. Thus an approximation can be expressed by

$$I_r = 1 + \mu \left(\frac{V}{V_o}\right) , \tag{34}$$

where the correction factor $\mu \leq 1$. If the probe is sheath-area-limited, μ is approximately $1.5\ P^{2/3}$. If the probe is orbital-motion-limited, μ is equal to 1. In intermediate cases the values of μ are obtained by equating the right side of Eq. (34) to a numerically determined solution and solving for μ. The value of μ in the intermediate region is given in Fig. 15 as a function of T/Nr^2 where $P = 7.51 \times 10^3\ T/Nr^2$.

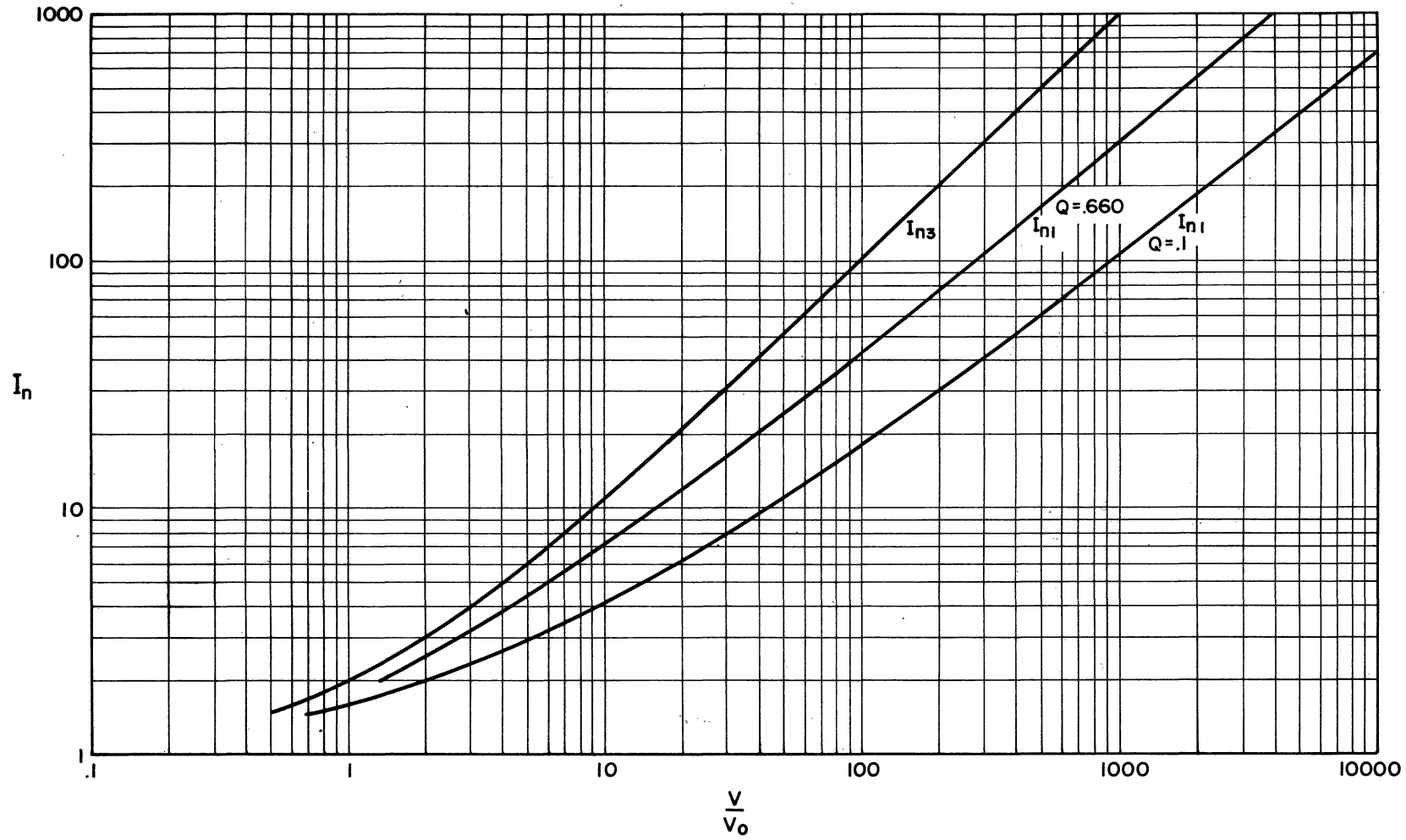

Fig. 14. Asymptotic solutions and numerical solution shown for comparison. I_{n1}, numerical solution; I_{n3}, orbital-motion-limited solution.

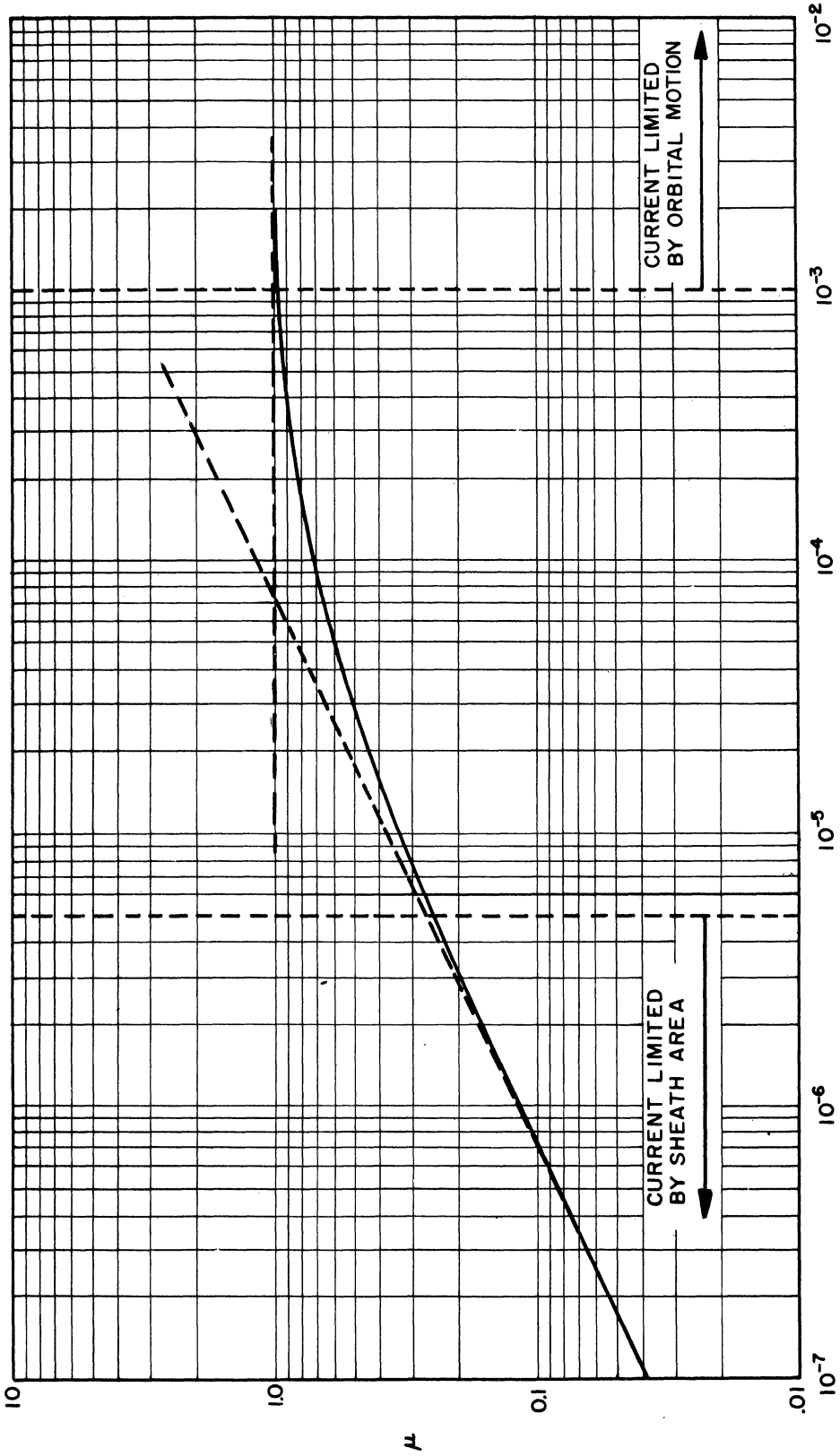

Fig. 15. Numerical values of μ for spherical electrode.

In the graphical presentation of μ vs. T/Nr^2, Fig. 15, the criteria for the sheath-area-limited and orbital-motion-limited cases become clear. Thus the electrode is sheath-area-limited if

$$\frac{T}{Nr^2} \leq 5 \times 10^{-6} \tag{35}$$

It is orbital-motion-limited if

$$\frac{T}{Nr^2} \geq 10^{-3} \tag{36}$$

In summation, while the general solution results in transcendental equations requiring either machine or graphical solution, there are several approximating equations which afford reasonable accuracy. Four methods of calculating the current to an electrode which has an accelerating potential for the particles, with respect to the plasma, are as follows.

1. General.—The numerical solution, which is the simultaneous solution of Eqs. (27) and (30) with the relations of a/r and $-\alpha^2$, either by machine or graphical means.

2. General.—An approximate solution which adapts the orbital-motion-limited solution, Eq. (32), for use in intermediate or sheath-area-limited cases.

3. Asymptotic.—The orbital-motion-limited solution, Eq. (32), when it applies.

4. Asymptotic.—The sheath-area-limited solution, Eq. (33), when it applies.

The various equations, both general and approximate, for sphere and cylinder and plane are tabulated in Table I. The choice between using the general equations or an approximate solution depends on the accuracy required. The appropriate choice of approximate solution may be based on consideration of the factor T/Nr^2, presented in Fig. 15 and appearing in Eqs. (35) and (36).

To aid in the choice of the most appropriate solution for a particular application, the numerical solution is compared in Fig. 16 with the approximate solution, and in Fig. 17, with the sheath-area-limited solution for 3 values of P. The values of (V/V_0) generally encountered in a practical application lie between 2 and 20.

TABLE I

PLASMA-IMMERSED-ELECTRODE CURRENTS

	Sphere	Cylinder	Plane
Retarding Potential, $V/V_o > 0$			
1. General Numerical	$I_n = \left(\frac{a}{r}\right)^2 - \left(\frac{a^2-r^2}{r^2}\right) \exp - \left(\frac{V}{V_o}\right)\left(\frac{r^2}{a^2-r^2}\right)$	$I_n = \frac{a}{r} \operatorname{erf}\left[\frac{r^2(V/V_o)}{a^2-r^2}\right]^{1/2} + \left\{1 - \operatorname{erf}\left[\frac{a^2(V/V_o)}{a^2-r^2}\right]^{1/2}\right\} \exp\left(\frac{V}{V_o}\right)$	$I_n = 1$
	$I_n = \frac{P}{-\alpha^2}\left(\frac{V}{V_o}\right)^{3/2}$	$I_n = \frac{P}{-\beta^2}\left(\frac{V}{V_o}\right)^{3/2}$	$I_n = \frac{8\sqrt{\pi}\,\epsilon_o\,kT}{9\,N\,e^2 s^2}\left(\frac{V}{V_o}\right)^{3/2}$
	where $P = \frac{8\sqrt{\pi}\,\epsilon_o\,kT}{9\,N\,e^2 r^2}$	$P = \frac{8\sqrt{\pi}\,\epsilon_o\,kT}{9\,N\,e^2 r^2}$; $\operatorname{erf} X = \frac{2}{\sqrt{\pi}}\int_o^X e^{-y^2}\,dy$	
2. General Approximate	$I_n = 1 + \mu_s\left(\frac{V}{V_o}\right)$	$I_n = \sqrt{1 + \mu_c(V/V_o)}$	$I_n = 1$
3. Asymptotic Orbital-Motion-Limited	$I_n = 1 + \left(\frac{V}{V_o}\right)$	$I_n = \sqrt{1 + (V/V_o)}$	$I_n = 1$
4. Asymptotic Sheath-Area-Limited	$I_n = \left(\frac{a}{r}\right)^2$	$I_n = \frac{a}{r}$	$I_n = 1$
Retarding Potential, $V/V_o < 0$			
	$I_n = \exp\left(\frac{V}{V_o}\right)$	$I_n = \exp\left(\frac{V}{V_o}\right)$	$I_n = \exp\left(\frac{V}{V_o}\right)$

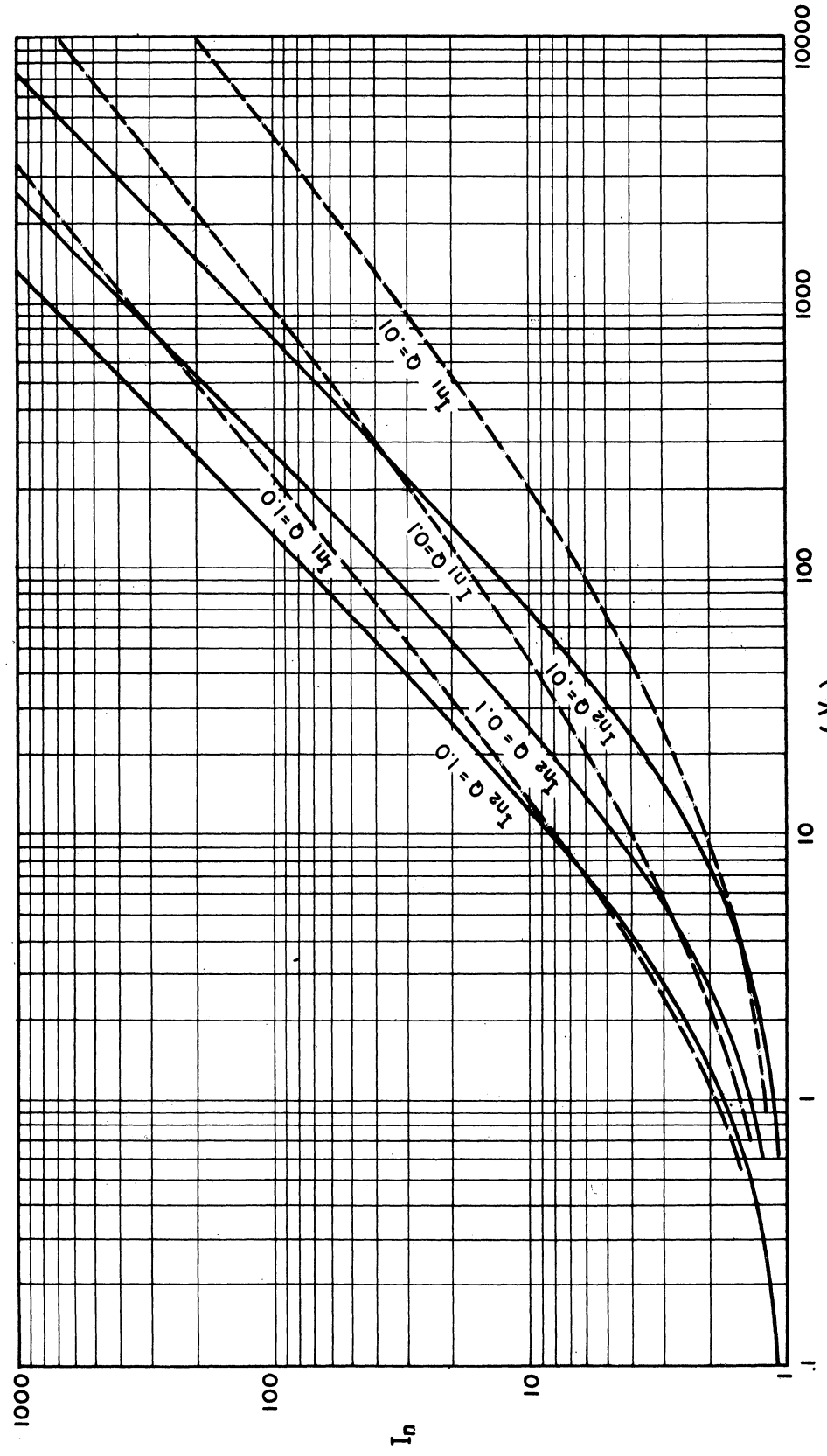

Fig. 16. Numerical (I_{n1}) and approximate (I_{n2}) solutions shown for comparison.

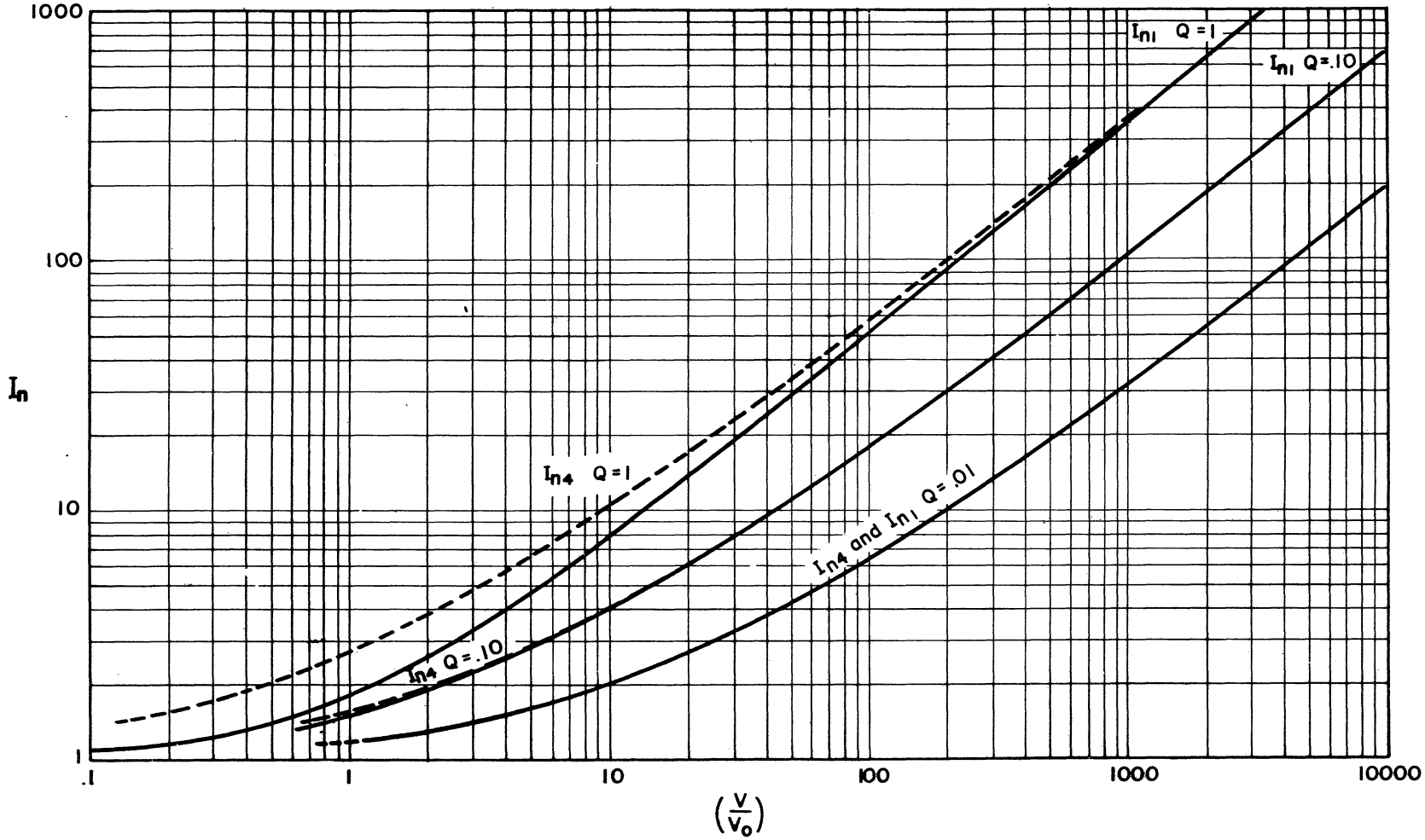

Fig. 17. Numerical (I_{n1}) and sheath-area-limited (I_{n4}) solutions shown for comparison.

IV. APPLICATION OF THEORETICAL DEVELOPMENT TO HYPOTHETICAL PROBES

A. SINGLE-ELECTRODE PROBE

The net current to an electrode in a plasma is composed of positive ions, negative ions, and electrons. Thus to obtain the net current it is necessary to add algebraically the individual currents calculated by the above equations.

The current to a single spherical electrode in a plasma containing only positive ions and electrons is shown in Fig. 18.

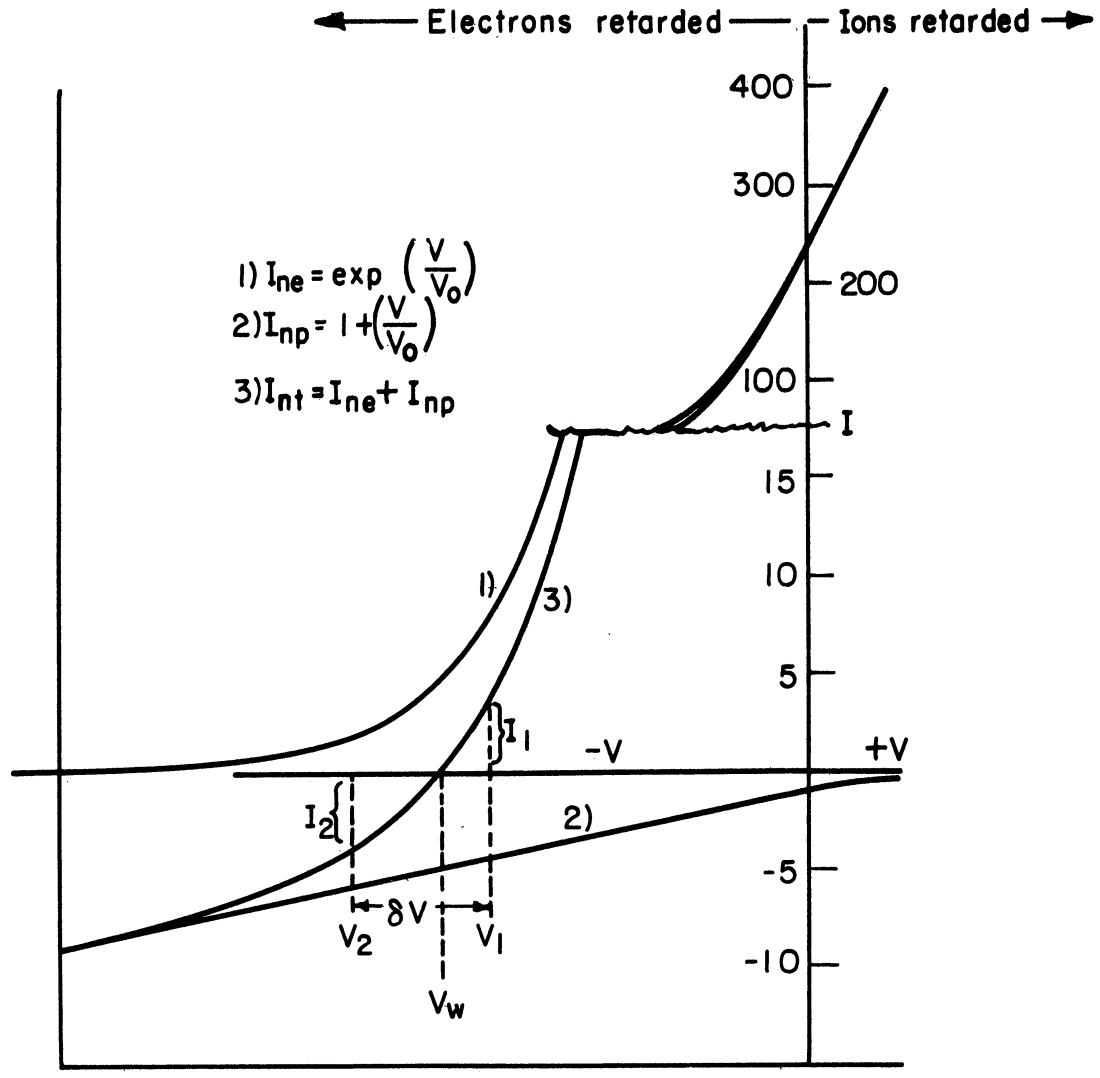

Fig. 18. Single spherical electrode volt-ampere characteristics.

Curve (1) is a sketch of electron current vs. voltage. Curve (2) shows orbital-motion-limited ion current Eq. (32) applies in this case. Curve (3) is the algebraic sum of curves (1) and (2); thus it is the net current to an individual electrode as a function of its voltage.

Experimentally, curve (3) (Fig. 18) is obtained by measuring the current resulting from applying a linearly changing voltage between the plasma-immersed electrode and a fixed reference. If this voltage reference is the cathode, as it usually is in laboratory applications, the applied voltage will be zero at some point to the left of V_w. The voltage between the reference voltage and the current axis of Fig. 18 is then called the plasma voltage, V_p.

B. BIPOLAR PROBE OF EQUAL AREA ELECTRODES

In the design of an ionosphere probe, no fixed reference is available. Even the entire carrier vehicle, in general, does not permit the assumption of a fixed reference. Thus, one must consider a two-electrode system, referred to herein as a bipolar probe, and must then recognize that the net current to the system from the plasma is zero except for transient effects.

Bipolar probes have been used to advantage in gas-discharge-tube studies as well as in the previously mentioned rocket instrumentations. In the former, they have proven to yield certain data with less disturbance of the plasma than a single-electrode probe.[10,11]

If two identical unconnected conducting spherical electrodes are immersed in a plasma, they will assume voltages with respect to the plasma such that the current to each is zero. This condition is depicted in Fig. 19, which shows a sketch of the voltage distribution along a line passing through the center of the spheres. Here each sphere is considered completely isolated in the plasma, no attempt being made to show the alterations of the voltage distribution due to a connecting lead (to be added) or the presence of the second sphere.

In practice, the two probes are connected by a voltage source which provides a linearly changing voltage as

$$\delta V = V_1 - V_2 \tag{37}$$

where V_1 is the voltage between electrode 1 and the plasma, and V_2 is the voltage between electrode 2 and the plasma. It is seen that, when δV is positive, probe 1 rises above V_w (wall potential) and draws an electron current. Simultaneously probe 2 will fall below V_w and draw an equal positive-ion current (see also Fig. 18). Only δV can be varied; V_1 and V_2 are determined by the properties of space to meet the requirement of zero net current.

In determining the characteristics of a bipolar probe, it is convenient to plot the current to the individual electrodes as shown in Fig. 20. Thus the

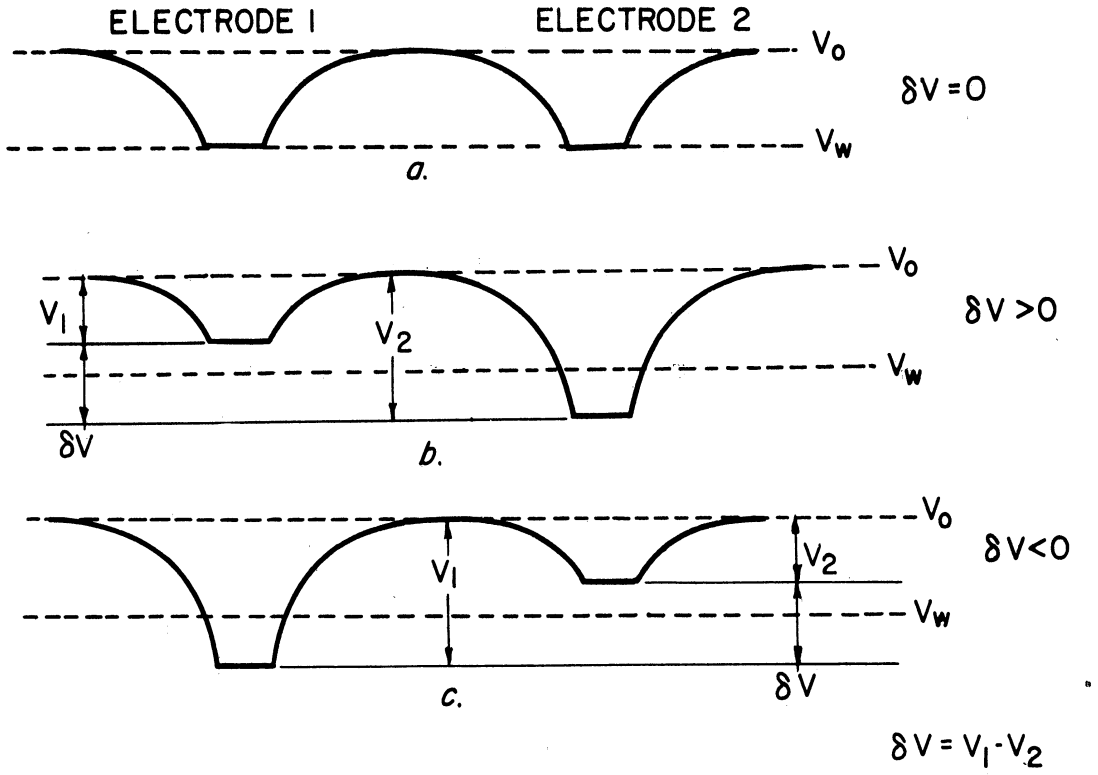

Fig. 19. Potential diagram of a bipolar probe.

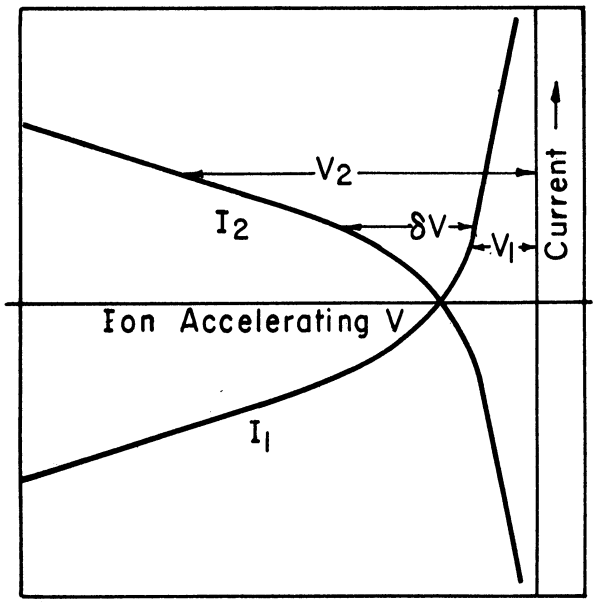

Fig. 20. Single spherical electrode volt-ampere characteristics.

volt-ampere characteristic of the particular probe pair can be determined by reading the voltage between the two curves for specific current values.

A typical curve so obtained is shown in Fig. 21. The letters on the curve indicate approximate boundaries of regions of particular interest. In the AB and EF

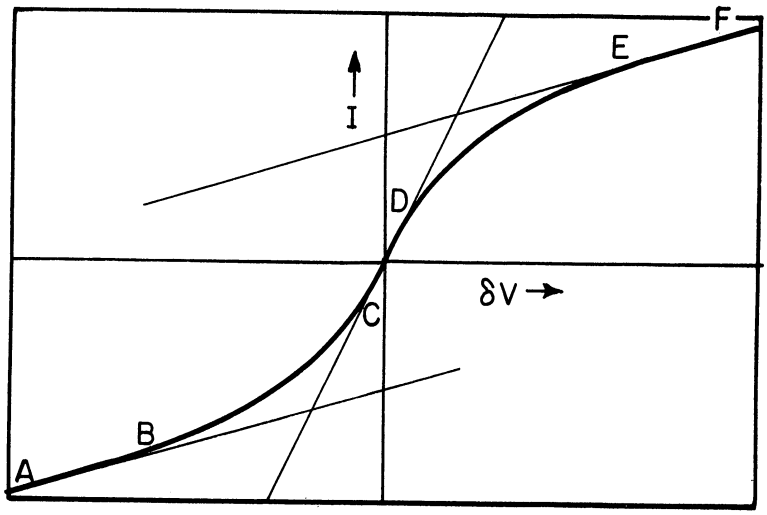

Fig. 21. Volt-ampere characteristic of a bipolar-equal-area probe.

regions, the electrode having a net electron flow ($V > V_w$) requires a relatively small change in potential for a large change in current; therefore the shape of the curve in this interval may be assumed to be determined entirely by the volt-ampere characteristics of the other electrode which is drawing a net positive-ion current. In the BC and DE regions the departure of the curve from the nearly straight line sections, AB and EF, is due to a change of the electron current to the electrode drawing a net positive-ion current.

In the CD region, both electrodes are approaching the wall potential. Thus the change in current to one is almost identical to the inverse of the change to the other, resulting in a near-linear characteristic in this region. The origin is the point of inflection of the symmetrical curves and is also the maximum slope of the bipolar volt-ampere characteristic. Given an experimental curve, the electron current can be determined by extending the AB portion of the curve to determine the difference in current between this extended curve and the curve in the BC region. This is a good approximation of the electron current drawn by probe 1. The electron current so determined is, for practical purposes, represented by Eq. (23). Since this equation is an exponential function of V/V_0 alone, it is seen that a plot of $\log_e i_e$ vs. voltage results in a straight line whose slope is the reciprocal of the voltage equivalent (V_T) of the electron temperature (Fig. 22).

The ion density may be obtained from such an experimental curve by utilizing the electron temperature as determined above and the AB or EF region of the curve.

A more complete discussion of data reduction and interpretation will be included in a report on the data obtained from the previously mentioned firings. The above are the simplest and most straightforward theoretical methods, but are not necessarily the most appropriate for the reduction of experimental data.

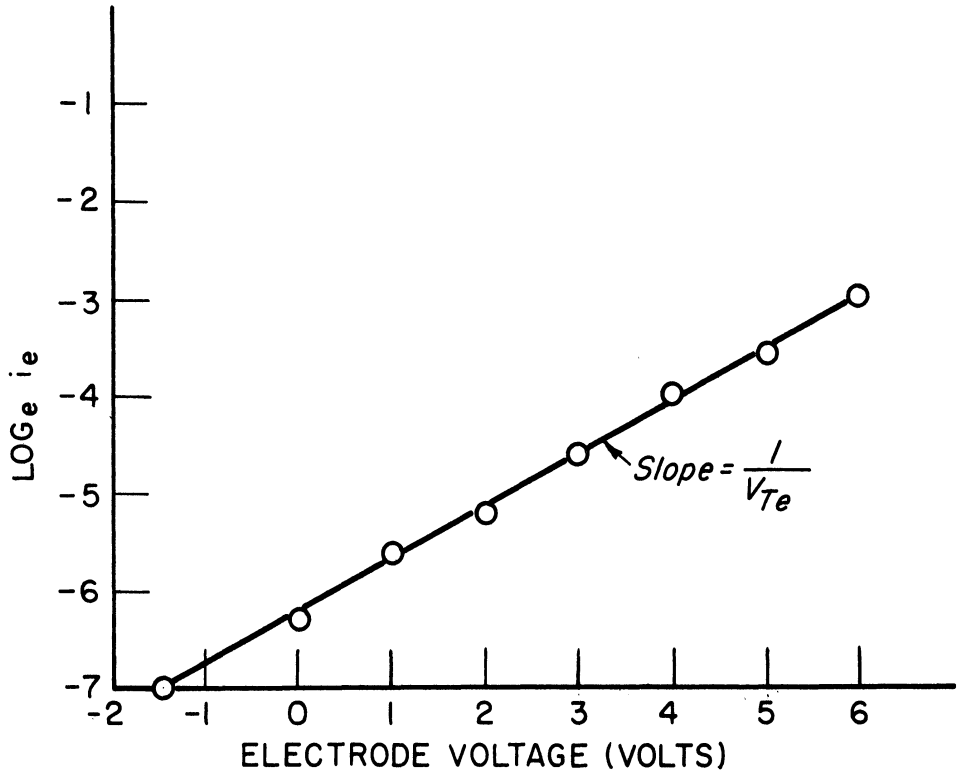

Fig. 22. $\text{Log}_e\ i_e$ vs. V, log electron current vs. electrode difference voltage.

C. BIPOLAR PROBE OF UNEQUAL AREA ELECTRODES

If the two electrodes of a bipolar probe are unequal in area, or if they have different geometries, the volt-ampere characteristic will not be symmetrical. If they have the same geometry but are unequal in area, and if the ion current to each electrode is limited in the same manner, the current between the electrodes, signal current, is approximately zero when δV is zero. This condition is illustrated in Fig. 23 for two orbital-motion-limited electrodes where $A_1/A_2 = 1/2$. (A_1 is the area of the number 1 electrode and A_2 is the area of the number 2 electrode.)

The higher current for a given V/V_0 occurs when the larger electrode is drawing positive-ion current, the smaller one drawing electron current. Unequal electrode systems sample a larger percentage of the electrons, thereby permitting electron energy distribution to be determined. This objective, however, would require greater area ratios than the 2-to-1 of the preceding example.

If the area ratio were great enough, the bipolar probe current would be limited by the electron flow to the smaller electrode rather than by the ion current to the larger. This would allow an independent measurement of ion temperature and electron density as well as energy distribution. However, more must be known about the physical processes taking place in the surrounding regions before the data from the electron-limited characteristic could be interpreted with confidence.

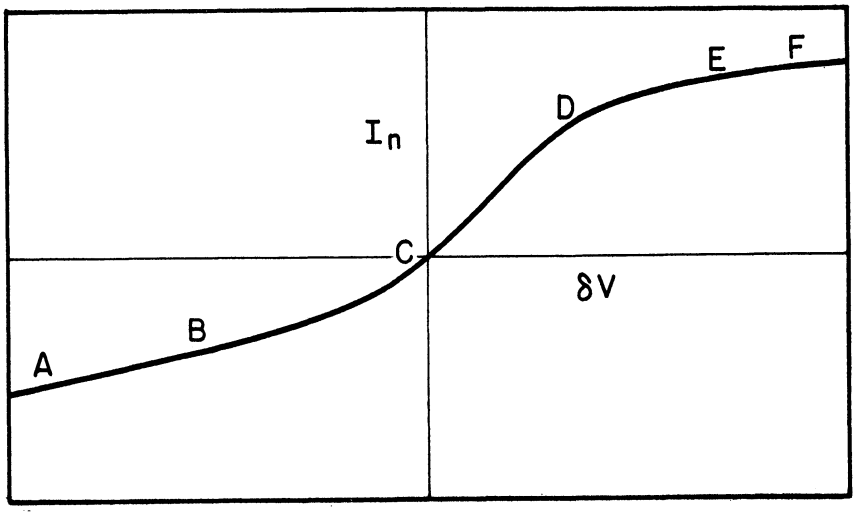

Fig. 23. Volt-ampere characteristics of unequal-area-bipolar probe.

If the shapes of the electrodes are not alike, or if an area difference results in current-limiting conditions differing for two similar geometry electrodes, the characteristic will not be symmetrical, nor will zero δV result in zero signal current. The δV resulting in zero signal current is a function of the area ratio, number density ratio, square root of temperature ratio, and square root of ion and electron mass ratio, and the geometry of the electrodes. For example, take two electrodes with an area ratio of 54 in a region of atomic oxygen ions, square root of mass ratio 171, and ion and electron temperatures and number densities equal. The smaller electrode is an "orbital-motion-limited" cylinder, and the larger electrode is a "sheath-area-limited" sphere. In Fig. 24 the single-electrode characteristic of the cylinder is shown as curve (1) and the

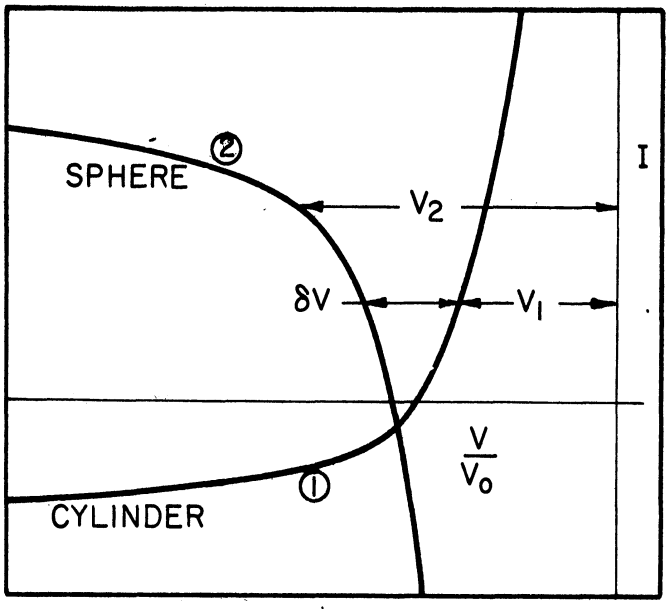

Fig. 24. Sphere and cylinder single-electrode volt-ampere characteristics.

single-electrode characteristic of the sphere is curve (2). The bipolar characteristic obtained from Fig. 24 is shown in Fig. 25. The AB region of this curve exhibits the ion current characteristic of the cylinder, and the EF region shows the ion current characteristic of the sphere. The difference between BC and AB

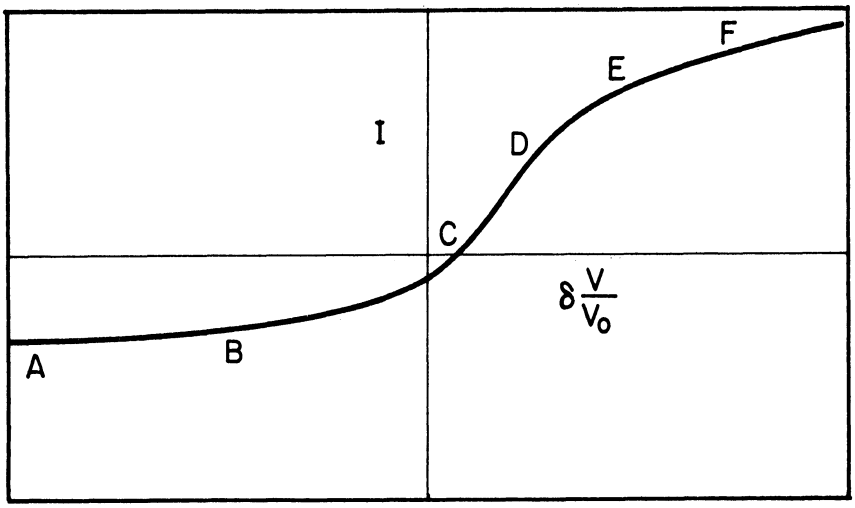

Fig. 25. Sphere-cylinder bipolar probe characteristic.

extended is the electron current to the cylinder, and the difference between DF and EF extended is the electron current to the sphere. The CD region is still a nearly linear section corresponding to the minimum impedance to space seen by the probe, but is no longer at the origin.

The characteristic of many other possible electrode combinations may be visualized once familiarity is gained with typical single-electrode solutions. However, caution must be exercised in anticipating the results of a particular combination since the equations are functions of V, and the characteristic is a function of δV, which is not linearly related to V. Figure 26 illustrates three typical solutions for a spherical probe, and Fig. 27 illustrates the orbital-motion-limited solutions for three commonly used geometries.

In summation, an ionosphere probe must be considered as a two- or more electrode system since, in general, no fixed reference voltage is available. "Orbital-motion-limited" electrodes are desirable because of their mathematical simplicity, but they also result in low currents due to their small size. In addition, the electrode system must contain the circuitry (current detectors, δV generators, telemetering, etc.). Thus at least one of the electrodes will be too large to be orbital-motion-limited. It is desirable that the electrodes have a simple geometry (sphere, cylinder, plane) and are of such size that the current may be expressed by one of the asymptotic forms. Thus at least one of the electrodes will be sheath-area-limited.

The relative size of the electrodes influences the bipolar characteristic. A large area ratio permits the study of electron energy distribution, which, if

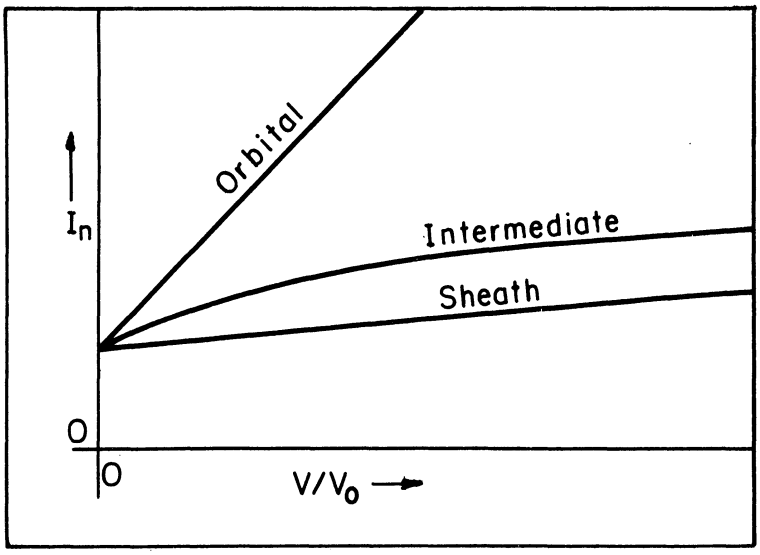

Fig. 26. Typical ion current characteristics, spherical electrode.

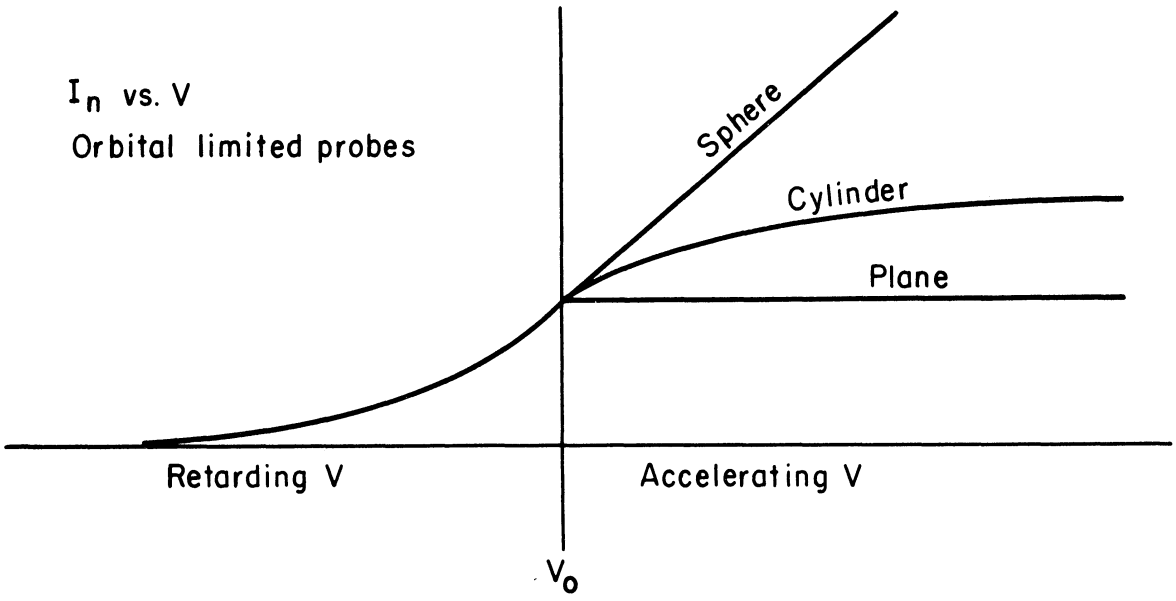

Fig. 27. Orbital-motion-limited electrode characteristics for sphere, cylinder, and plane.

high enough, permits an independent measurement of the electron density and ion temperature.

In addition to the two-electrode systems discussed, multiple-electrode systems might prove more useful in satellite applications.[12] Screened electrodes also have been used to advantage when the instrumentation was not ejected.[13] Another technique which might be employed is the use of a radioactive material

as a variable current source in lieu of a large-area second electrode. The δV would then become the measured quantity.

V. CONCLUSION

It has been shown that the current to a conducting electrode immersed in an ionized region such as the ionosphere depends on several properties of the region, including (1) electron temperature, (2) electron density, (3) ion density, (4) ion temperature, and (5) the effective ion mass. If, in some manner, the potential of the electrode is varied, the resulting volt-ampere curve also depends on the geometry, and, if bipolar, the characteristic depends on the electrode area ratio. The interdependence of the various factors has been outlined so that the volt-ampere characteristic of a sphere, cylinder, or plane, or combination of these, can be calculated.

The equations, however, are based on assumptions which are, in some cases, questionable, because many of the ionospheric properties are not adequately known. The energy-distribution assumption, for example, is one of these. Related to this is the nature of particle diffusion between the sheath and the undisturbed plasma, which has been assumed to be governed by the Boltzmann relation. This may not be an entirely suitable approximation. Significant use of the probe technique does not, however, require full knowledge of the validity of these assumptions. For this reason, experimental studies are being carried out with the objectives of (a) testing the theoretical treatment, and (b) Measuring ionospheric parameters.

Several additional factors, which can only be listed here, arise in the development of an ionosphere experiment:

(1) the effect of overlapping sheaths, which has been avoided through use of guard rings;

(2) gas contamination of the environment, which has been avoided through separation of the rocket and the sealed probe instrumentation;

(3) disturbance of the ionosphere by the rf field of the telemeter, which has been investigated by making measurements with and without the transmitter operating;

(4) relative velocity of probe and ionosphere, whose effect has been minimized by choice of a symmetrical geometry and minimum horizontal rocket velocity; and

(5) thermoelectric, photoelectric, and contact potential effects, which have been minimized through consideration of materials and cleanliness.

After studying various electrode configurations, one simple configuration seemed most consistent with the objectives outlined above, construction possibilities, and the size and weight capabilities of the rockets available and anticipated. This probe (Fig. 28) was composed of two 6-in.-OD spheres separated by a 2-1/4-in.-OD cylindrical section 10 in. long. The outer hemispherical sections were insulated from the funnel-shaped inner sections. Only the volt-ampere characteristic of the outer hemispheres was telemetered, the funnel sections acting as guard electrodes.

This geometry with equal-area electrodes is particularly suited for measuring electron temperature. In addition, measurement of the ion density and the minimum probe impedance to space is available. The disturbances mentioned above and certain other performance details pertain more to circuitry than to the subject of this report, and are discussed in detail in a separate report on the instrumentation.[14]

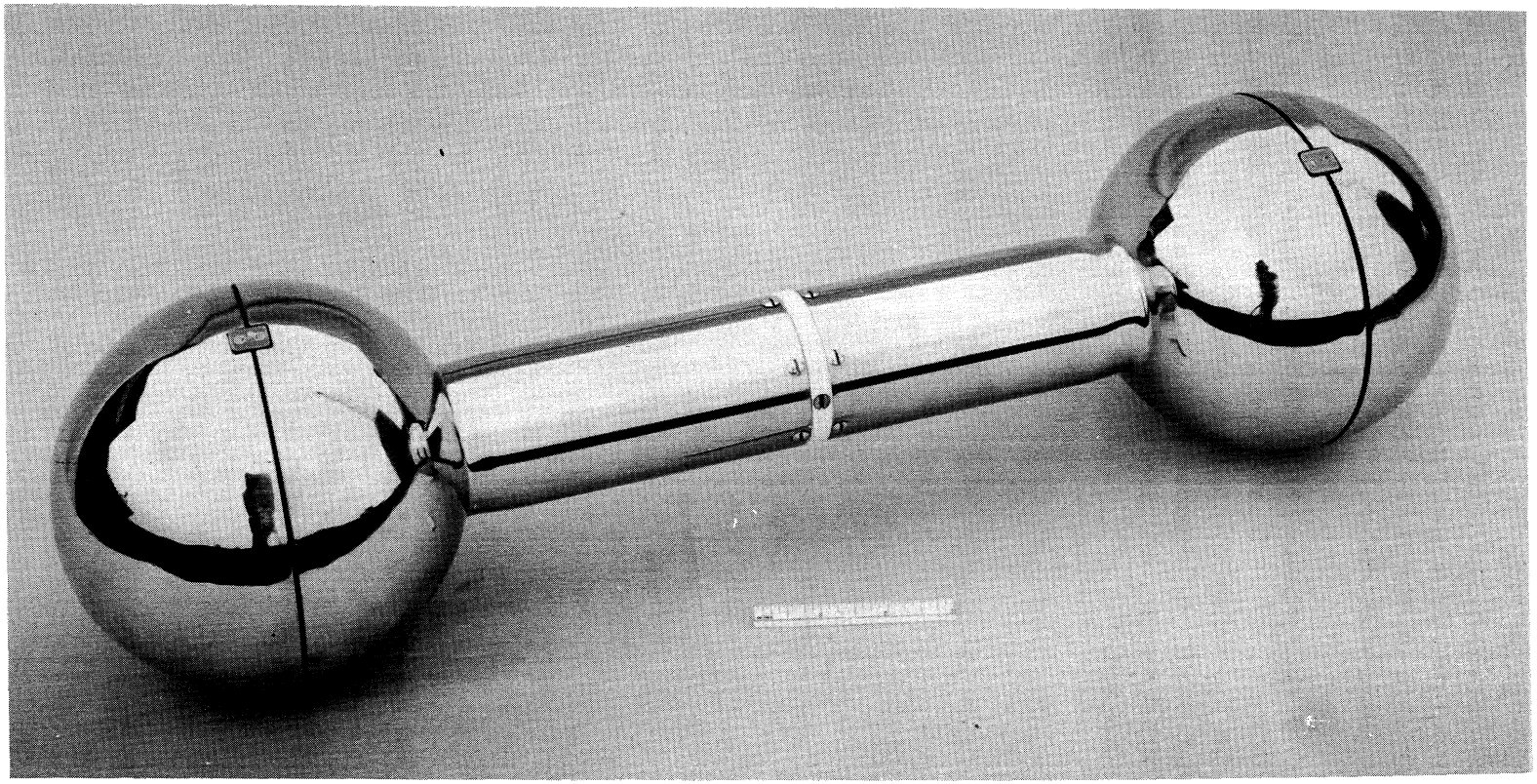

Fig. 28. Experimental model of double-sphere probe as employed for initial experiment.

VI. REFERENCES

1. Seddon, J. C., Pickar, A. D., and Jackson, J. E., "Continuous Electron Density Measurements up to 200 Km," J. Geophys. Res., 59, No. 4 (December, 1954).

2. Seddon, J. C., "Electron Densities in the Ionosphere," J. Geophys. Res., 59, No. 4 (December, 1954).

3. Seddon, J. C., and Jackson, J. E., "Absence of Bifurcation in the E-Layer," Phys. Rev., 97, 1182-1183 (February 15, 1955).

4. Jackson, J. E., "A New Method for Obtaining Electron-Density Profiles from P'-f Records," J. Geophys. Res., 61, No. 1 (March, 1956).

5. Hok, G., et al., Dynamic Probe Measurements in the Ionosphere, Univ. of Mich. Eng. Res. Inst. Report, Ann Arbor, August, 1951. Reprinted as Univ. of Mich. Res. Inst. Report 2521-5-S, AFCRC TN-58-616.

6. Hok, G., Spencer, N. W., and Dow, W. G., "Dynamic Probe Measurements in the Ionosphere," J. Geophys. Res., 58, No. 2 (June, 1953).

7. Reifman, A., and Dow, W. G., "Theory and Application of the Variable Voltage Probe for Exploration of the Ionosphere," Phys. Rev., 75, 1311A (1949).

8. Reifman, A., and Dow, W. G., "Dynamic Probe Measurements in the Ionosphere," Phys. Rev., 76, 987 (1949).

9. Langmuir, I., and Mott-Smith, H., Jr., "Studies of Electric Discharges in Gases at Low Pressures," Gen. Electrical Rev.; Part I, 27, No. 7 (July, 1924); Part II, 27, No. 8 (August, 1924); Part III, 27, No. 9 (September, 1924).

10. Johnson, E. O., and Malter, L., "A Floating Double Probe Method for Measurements in Gas Discharges," Phys. Rev., 80, 58-68 (October, 1950).

11. Koyiuna, S., and Takayana, K., J. Phys. Soc. Japan, 4, 349 (1949).

12. Hok, G., Sicinski, H. S., and Spencer, N. W., "Temperature and Electron-Density Measurements in the Ionosphere by a Langmuir Probe," Scientific Uses of Earth Satellites, ed. by J. A. Van Allen, The University of Michigan Press, Ann Arbor, 1956.

13. Krassovsky, V. I., "Exploration of the Upper Atmosphere with the Help of the Third Soviet Sputnik," presented at the International Astronautical Federation Congress in Amsterdam, August, 1958.

14. Spencer, N. W., Bi-Polar Instrumentation No. 1, Univ. of Mich. Res. Inst. Report 2521, 2618:1-1-S (FS-1), Ann Arbor, October, 1958 (AFCRC TN-58-617).